Electronic Supplementary Material (ESI) for Organic & Biomolecular Chemistry.


# Supporting information

## A direct entry to polycyclic quinoxaline derivatives via $I_2$-DMSO mediated oxidative decarboxylation of α-amino acids and subsequent Pictet-Spengler cyclization reaction

Surya Kanta Samanta,[a] Rumpa Sarkar,[a] Utsav Sengupta,[a] Sayan Das[b], Debabani Ganguly,[b] Avantika Hasija,[c] Deepak Chopra[c] and Mrinal K. Bera*[a]

[a]Department of Chemistry, Indian Institute of Engineering Science and Technol1ogy (IIEST), Shibpur, Howrah- 711 103 (WB), India

[b]Centre for Health Science and Technology, JIS Institute of Advanced Studies and Research, JIS University, Kolkata, India

[c]Crystallography and Crystal Chemistry Laboratory, Department of Chemistry, Indian Institute of Science Education and Research Bhopal, Bhopal- 462066, India

## Table of Contents

**A. General Methods :**

All reactions were performed under an atmosphere of nitrogen in oven-dried flasks. TLC was performed on pre-coated silica gel plates. TLC plates were visualized under UV light at 254 nm and iodine vapour. $^{1}H$ NMR spectra were recorded on Bruker 400 MHz and $^{13}C$ NMR spectra were recorded on a Bruker 100 MHz spectrometer using $CDCl_3$ and DMSO-$d_6$ as a solvent with TMS as the internal standard. The chemical shifts value at 7.26 and 77.0 ppm are referenced for $CDCl_3$ solvent. The data of HRMS was carried out on a high-resolution mass spectrometer instrument. X-ray structural analysis was conducted by Bruker D8-Venture X-ray analysis instrument. All the commercial reagents were used from different commercial sources without further purification.

**B. Screening of the reaction**

**Table 1.** Preliminary screening of decarboxylative cyclisation reaction[a]

| Entry | Iodine source (equiv) | Additives | Solvent | Yield (%) |
|---|---|---|---|---|
| 1 | $I_2$ (0.1) | TFA | DMSO | ND |
| 2 | $I_2$ (0.5) | TFA | DMSO | 13 |
| 3 | $I_2$ (1.0) | TFA | DMSO | 74 |
| 4[b] | $I_2$ (1.0) | TFA | DMSO | 72 |
| 5 | $I_2$ (1.5) | TFA | DMSO | 70 |
| 6 | $I_2$ (1.0) | HI | DMSO | 58 |
| 7 | $I_2$ (1.0) | AcOH | DMSO | 62 |
| 8 | $I_2$ (1.0) | HCl | DMSO | 48 |
| 9 | $I_2$ (1.0) | TsOH | DMSO | 34 |
| **10** | $I_2$ (1.0) | **TFA** | **DMSO:$H_2O$** | **90** |
| 11 | $I_2$ (1.0) | AcOH | DMSO:$H_2O$ | 70 |
| 12 | $I_2$ (1.0) | HCl | DMSO:$H_2O$ | 76 |
| 13 | $I_2$ (1.0) | TFA | DMF | ND |
| 14 | $I_2$ (1.0) | TFA | $CH_3CN$ | ND |
| 15 | KI | TFA | DMSO | ND |
| 16 | NIS | TFA | DMSO | ND |

[a] Reaction condition: **1a** (1.0 equiv), **2a** (1.5 equiv), $I_2$ (100 mol%), Trifluroacetic acid (1.0 equiv), DMSO:$H_2O$ (9:1), $100^0$C (10-12 hr). [b] Reaction is carried out at $120^0$C.

## C. General Procedure for the synthesis of *N*-hetrocycles 3a and other *N*-hetrocycles

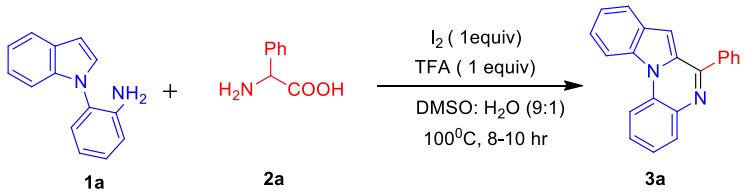


A 30 ml sealed tube was charged with Phenyl glycine **2a** (227 mg, 1.5 mmol), DMSO: $H_2O$ (9:1) 3 ml and iodine (254 mg, 1 mmol) and Trifluoroacetic acid (0.17 ml, 1 mmol) and the mixture was stirred for half an hour at room temperature. After that 2-(1*H*-indol-1-yl)aniline **1a** (208 mg, 1.0 mmol) was added and the resulting reaction mixture was heated to $120^0$C for 10-12 hr. After completion of the reaction as indicated by TLC, the reaction flask was cooled for a while. After that 10% aqueous $Na_2S_2O_3$ solution (30 mL) and saturated aqueous $NaHCO_3$ solution were added. The whole reaction mixture was extracted with ethyl acetate (3×60 mL). The combined organic layer was washed with brine solution and dried over anhydrous $Na_2SO_4$ and concentrated under reduced pressure. The crude product was purified via column chromatography (100-200 mesh silica gel) with petroleum ether and ethyl acetate (20% of solution) as eluent to yield the desired product **3a** as yellow solid (265 mg, yield 90%). Also, other derivatives of *N*-heterocycles **3b- 3l, 4a-4h** and **6a-6d** were synthesized by the above procedure in good to moderate yield.

## D. X-ray crystallographic data

Single crystals of **3e** and **3l** were obtained by slow evaporation from a solution of ethyl acetate and hexane (3:7). Data were collected using Bruker D8-Venture diffractometer. Further information was available from Cambridge crystallographic data center (UK) with CCDC deposition numbers **2155170** and **2048680**.

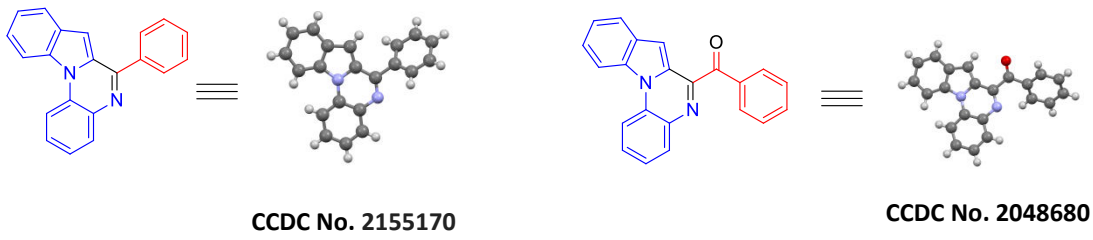


**Fig. 1** ORTEP diagram of the compound **3e** and **3l** with at 50 % probability level.

**Table 3: Crystallographic data and structure refinement parameter for 3e**

Identification code : **3e**

Molecular Weight : 294.3493

Bond precision: C-C = 0.0116 A Wavelength=0.71073

Cell: a=4.0812(8) b=17.973(3) c=19.807(4)
alpha=90 beta=90 gamma=90

Temperature: 293 K

| | Calculated | Reported |
|---|---|---|
| Volume | 1452.9(5) | 1452.9(5) |
| Space group | P 21 21 21 | P 21 21 21 |
| Hall group | P 2ac 2ab | P 2ac 2ab |
| Moiety formula | C21 H14 N2 | C21 H14 N2 |
| Sum formula | C21 H14 N2 | C21 H14 N2 |
| Mr | 294.34 | 294.34 |
| Dx,g cm-3 | 1.346 | 1.346 |
| Z | 4 | 4 |
| Mu (mm-1) | 0.080 | 0.080 |
| F000 | 616.0 | 616.0 |
| F000’ | 616.21 | |
| h,k,lmax | 4,21,23 | 4,21,23 |
| Nref | 2647[ 1599] | 2645 |
| Tmin,Tmax | 0.976,0.980 | 0.569,0.746 |
| Tmin’ | 0.976 | |

Correction method= # Reported T Limits: Tmin=0.569 Tmax=0.746 AbsCorr = MULTI-SCAN

Data completeness= 1.65/1.00 Theta(max)= 25.332

R(reflections)= 0.0981( 2037) wR2(reflections)= 0.2696( 2645)

S = 1.102 Npar= 208

**Table 2: Crystallographic data and structure refinement parameter for 3l**

Identification code : **3l**

Molecular Weight : 322.1106

Bond precision: C-C = 0.0030 A Wavelength=0.71073

Cell: a=3.8833(4) b=16.3577(13) c=23.692(2)
alpha=90 beta=90.160(4) gamma=90

Temperature: 100 K

| | Calculated | Reported |
|---|---|---|
| Volume | 1505.0(2) | 1505.0(2) |
| Space group | P 21/c | P 1 21/c 1 |
| Hall group | -P 2ybc | -P 2ybc |
| Moiety formula | C22 H14 N2 O | C22 H14 N2 O |
| Sum formula | C22 H14 N2 O | C22 H14 N2 O |
| Mr | 322.35 | 322.35 |
| Dx,g cm-3 | 1.423 | 1.423 |
| Z | 4 | 4 |
| Mu (mm-1) | 0.089 | 0.089 |
| F000 | 672.0 | 672.0 |
| F000' | 672.26 | |
| h,k,lmax | 4,20,30 | 4,20,30 |
| Nref | 3225 | 3205 |
| Tmin,Tmax | 0.983,0.994 | 0.611,0.745 |
| Tmin' | 0.931 | |

Correction method= # Reported T Limits: Tmin=0.611
Tmax=0.745 AbsCorr = MULTI-SCAN

Data completeness= 0.994 Theta(max)= 26.896

R(reflections)= 0.0609( 2004) wR2(reflections)= 0.1229( 3205)

S = 1.028 Npar= 226

**E. Photophysical properties of 3f, 3g and 3j**

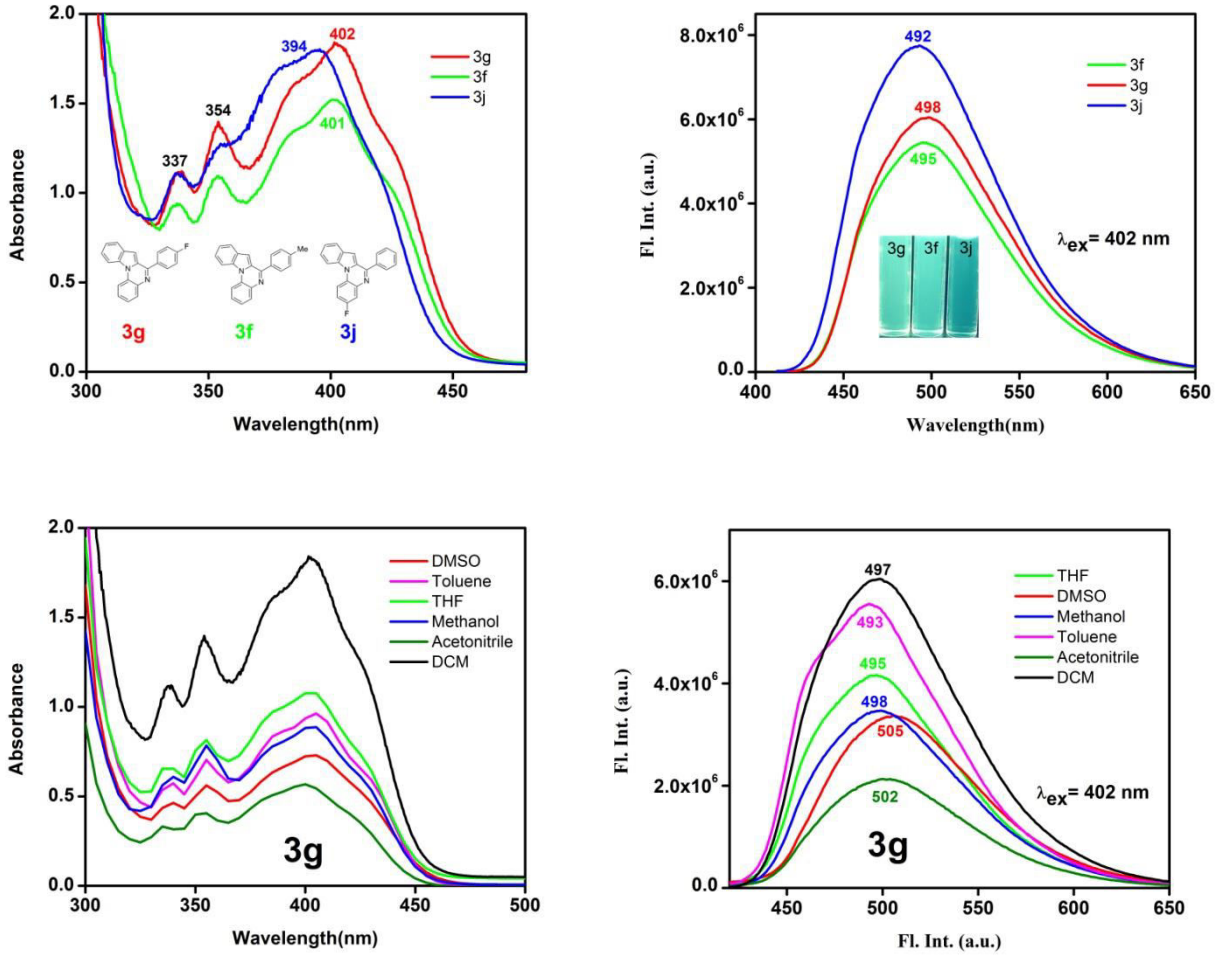


**Fig. 2** a) Normalised absorption spectra and b) fluorescence emission spectra of compounds **3f**, **3g**, **3j** in dichloromethane solvent (1× $10^{-6}$ M), c) Normalised absorption spectra of **3g** and d) Fluorescence emission spectra in different solvents with a concentration (1× $10^{-6}$ M) at excitation of 402 nm. Inset : photograph of **3f, 3g, 3j** under UV lamp (365 nm).

To our delight, we have found that three indoloquinaxaline derivatives **3f**, **3g**, **3j** show cyan color under UV light. Thus it is important to study the photophysical properties of these compounds via UV-visible and photoluminescence spectroscopic techniques. At first typical absorption and emission spectral data were recorded in DCM solvent (1.11 mM) as shown in Fig. 3 a) & b). In the UV-Vis spectra, these compounds show common peaks at 337 and 354 nm (may be due to n-π* transition from N atom to indoloquinaxaline moiety). But highest absorptions occur due to π- π* transitions of the conjugated systems for all of them. Here due to the strong electron-withdrawing effect of the Fluorine atom in the indoloquinaxaline ring of 3j, a blue shift occurs (as $\lambda_{max}$ appears at 394 nm) whereas for **3f** & **3g** substituents (R= -Me &-F) are far from the ring. The emission spectra of **3f**, **3g**, **3j** show $\lambda_{em}$ in the range

between 492-498 nm (**Fig. 3b**), and here also the presence of fluorine atom makes little influence leading to a certain blue shift (in **3j**) on emission wavelengths same as absorption curve. Then we have taken **3g** compound which shows solvent polarity dependent UV-Vis & fluorescence properties as shown in **Fig. 3(c-d)**. Here we can observe that with the increase in polarity of the solvents, redshift occurs in the emission spectrum[1]. Also in the polar aprotic solvents like DMSO and acetonitrile, the compound shows emission at a higher wavelength (505 & 502 respectively) but in non-polar toluene and less polar THF solvent, it gives peak at lower wavelength (493 & 495 respectively). A point to be mentioned is that in highly polar methanol, the emission peak of **3g** doesn't appear as high λ value as expected(498 nm). This can be due to the very low solubility of the compound in that solvent. All of these observations suggest that such indolo[1,2-*a*]quinoxalines derivatives could be promising biosensors and can be used in pharmaceutical industries as a large-scale application.

**References:**


1. Y. Zhang, W. Xiong, L. Chen, Y. Shao, R. Li, Z. Chen, J. Ge, N. Lv and J. Chen, *Org. Chem. Front.*, 2021, **8**, 304–309.


**F. Computational studies**

**Molecular Docking studies of compounds 3g, 3l and 3k**

**Table 1:** Derivatives of indoloquinoxaline used to check binding interactions with certain proteins.

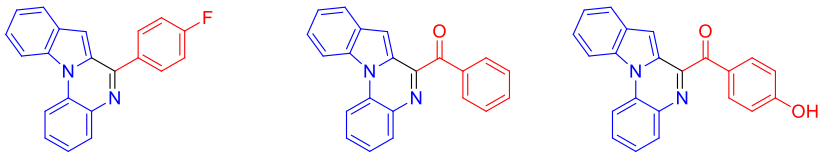


**3g** **3l** **3k**

To understand the role of the above derivatives (compounds **3g, 3l** and **3k**, of Table 1) as prospective drugs we have studied the binding interaction of the same with some selected targets. As reported earlier[1], indoloquinoxaline derivatives show anti-HIV properties. The HIV-1 protease leads to the replication of HIV where cleaves polypeptide chains to form functional proteins. HIV-1 protease inhibitors are immensely important drugs in antiretroviral treatments. To check how the above-mentioned derivatives of indoloquinoxaline interact, the X-ray crystal structure of the HIV-1 protease (PDB code: 6OGP, resolution: 1.53Å)[2] has been used as a model of the enzyme for docking. The downloaded PDB structure (monomer) from www.rcsb.org contains a ligand, the position of which has been used to determine the

binding site residues of the protein for computational docking. The Avogadro an open-source molecular builder and visualization tool, version 1.2.0[3] has been used to create and optimize the 3D structure of the derivatives to dock to the binding site of HIV-1 protease using AutoDock Vina.[4].The most stable pose of the ligand in the protein's binding site has the highest docking score. AutodockVina has also calculated the binding affinity of the acceptable protein-binding pose of the ligand. Here we are presenting the best ligand-protein conformation based on the highest docking score. SwissADME (www.swissadme.ch/) server has been used to calculate the physicochemical properties of each compound. The SMILES string of each compound was entered as input to generate the properties namely physicochemical properties, lipophilicity, water solubility, pharmacokinetics and drug likeness[5].

As per the docking result, **3g** (Table 1) has highest binding affinity. However, **3l** and **3k** are very close to the **3g** towards the protein binding. The binding site of the protein is mostly hydrophobic in nature, **3l** and **3k** are forming a single hydrogen bond between respective carbonyl oxygen and hydroxyl hydrogen of Thr80 of protein. Among these three molecules total polar surface area (TPSA) of **3g** is the least, 18.55Å$^{2,}$ (Table 4) and the hydrophobicity is the most as reflected from the highest LogP value, the measure of lipophilicity, (Table 4) of ADME analysis (http://swissadme.ch/index.php). Thus the binding of **3g** is driven by hydrophobic interactions.

**Table 2:** Binding affinity (kcal/mol) of compounds calculated from AutoDock Vina tool while binding HIV-1 protease. Only first mode of the ligand in the binding site is showing here.

| Compound | Mode | Binding affinity (kcal/mol) |
|---|---|---|
| **3g** | 1 | -9.7 |
| **3l** | 1 | -9.4 |
| **3k** | 1 | -9.2 |

**Table 3:** Binding parameters for the best binding pose of the ligand calculated at 298.15K

| Compound | Rank/Run | Estimated free energy of binding (kcal/mol) | Estimated inhibition constant (μM) | Cluster rmsd/ref rmsd (Å) |
|---|---|---|---|---|
| **3g** | 1/2 | -7.94 | 1.51 | 0.00/14.26 |
| **3l** | 1/10 | -8.51 | 0.57603 | 0.00/15.24 |
| **3k** | 1/2 | -8.34 | 0.77653 | 0.00/13.87 |

**Table 4:** ADME analysis

| Compound | TPSA (Å$^2$) | Log $P_{o/w}$ | Water solubility Log S (SILICOS-IT) | No. of H-bond acceptors/donors | Druglikeness | |
|---|---|---|---|---|---|---|
| | | | | | Lipinski | Bioavailibility score |
| **3g** | 18.55 | 4.64 | Poorly soluble | 1/1 | Yes, 1 violation | 0.55 |
| **3l** | 35.62 | 4.05 | Poorly soluble | 1/1 | Yes, 0 violation | 0.55 |
| **3k** | 55.85 | 3.59 | Poorly soluble | 2/2 | Yes, 0 violation | 0.55 |

TPSA: Topological polar surface area

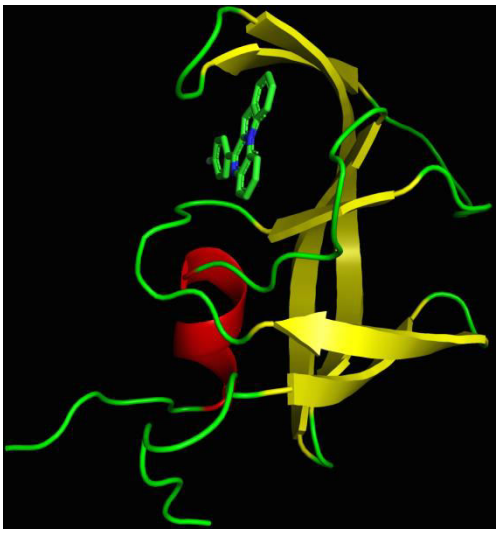

**Fig. 3** Binding of **3g** at protein's binding site. The ligand is hydrogen bonded to Gly48 residue of the protein.

**Fig. 4** Binding of **3l** at protein's binding site. The ligand is hydrogen bonded to Thr80 residue of the protein.

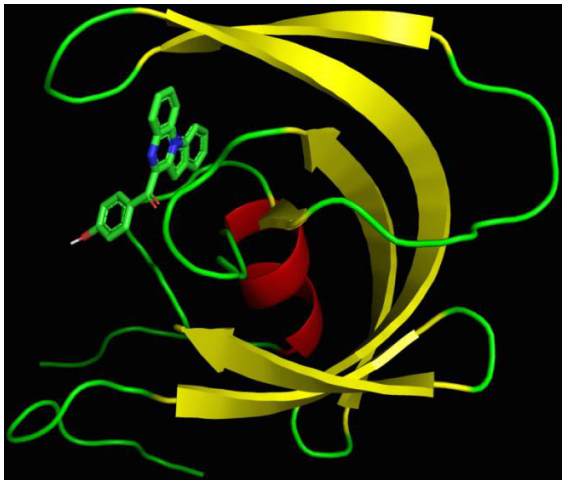

**Fig. 5** Binding of **3k** at protein's binding site. The ligand is hydrogen bonded to Thr80 residue of the protein.

**Refrences :**


1. L.-L. Fan, N. Huang, R.-G. Yang, S.-Z. He, L.-M. Yang and H. X. and Y.-T. Zheng, *Lett. Drug Des. Discov.*, 2012, **9**, 44–47.
2. H. Bulut, S. Hattori, H. Aoki-Ogata, H. Hayashi, D. Das, M. Aoki, D. A. Davis, K. V. Rao, P. R. Nyalapatla, A. K. Ghosh and H. Mitsuya, *Sci. Rep.*, 2020, **10**, 10664.
3. M. D. Hanwell, D. E. Curtis, D. C. Lonie, T. Vandermeersch, E. Zurek and G. R. Hutchison, *J. Cheminform.*, 2012, **4**, 17.
4. O. Trott and A. J. Olson, *J. Comput. Chem.*, 2010, **31**, 455–461.
5. A. Daina, O. Michielin and V. Zoete, *Sci. Rep.*, 2017, **7**, 42717.

## H. Copies of $^{1}H$ NMR and $^{13}C$ NMR compounds :

### 6-methylindolo[1,2-*a*]quinoxaline (3a) :

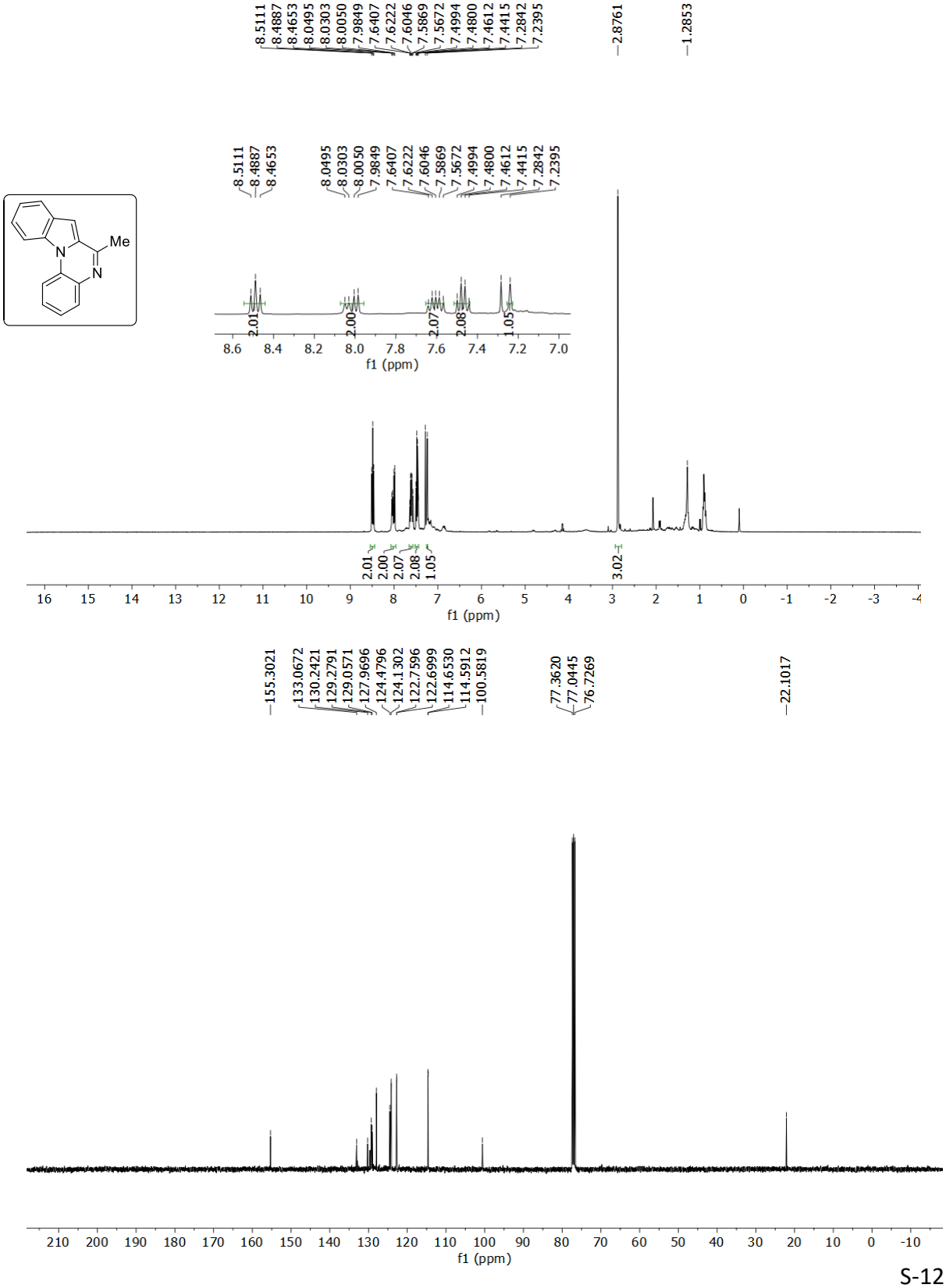

**7-(methylthio)indolo[1,2-*a*]quinoxaline (3b) :**

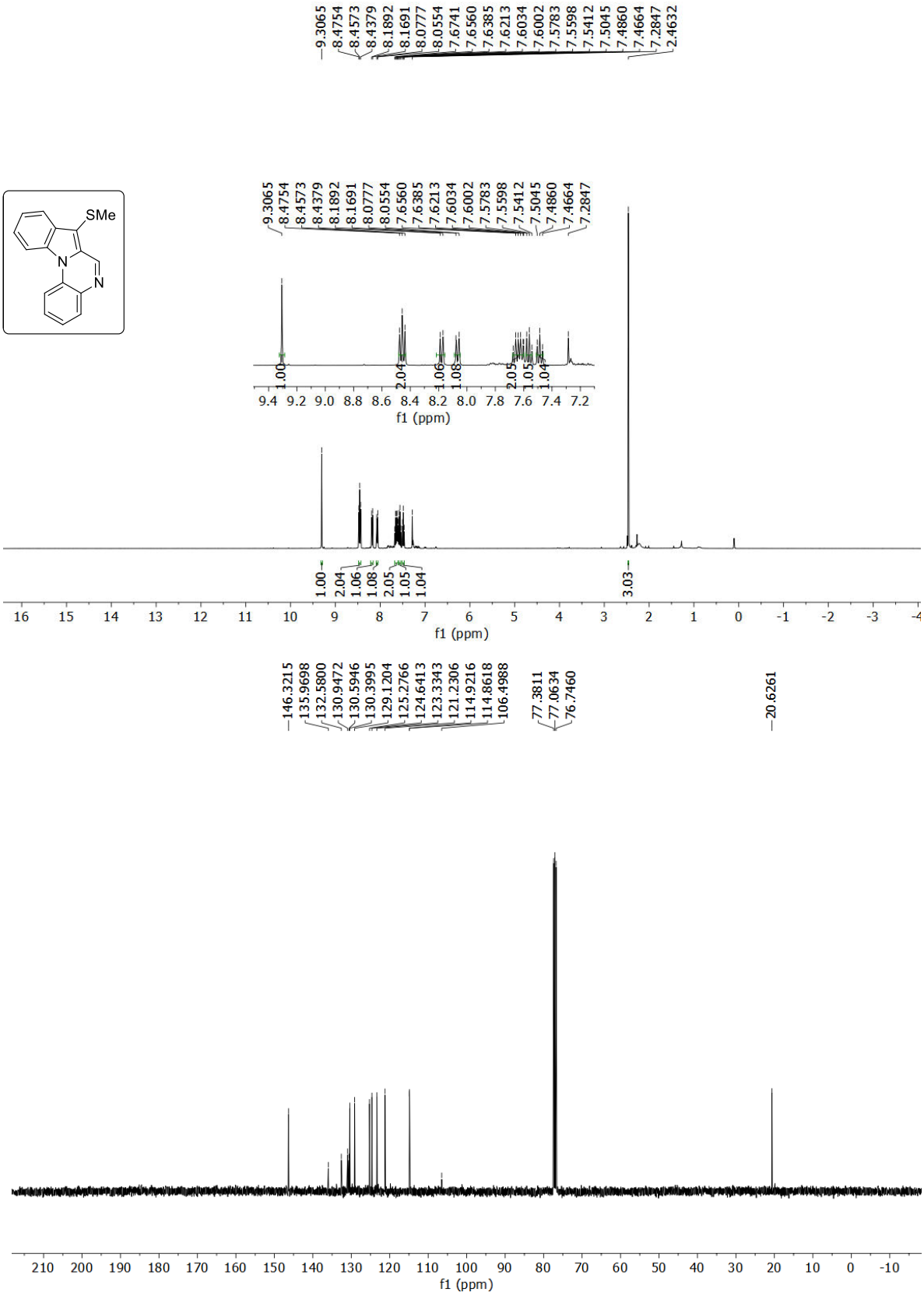

**6-isopropylindolo[1,2-*a*]quinoxaline (3c) :**

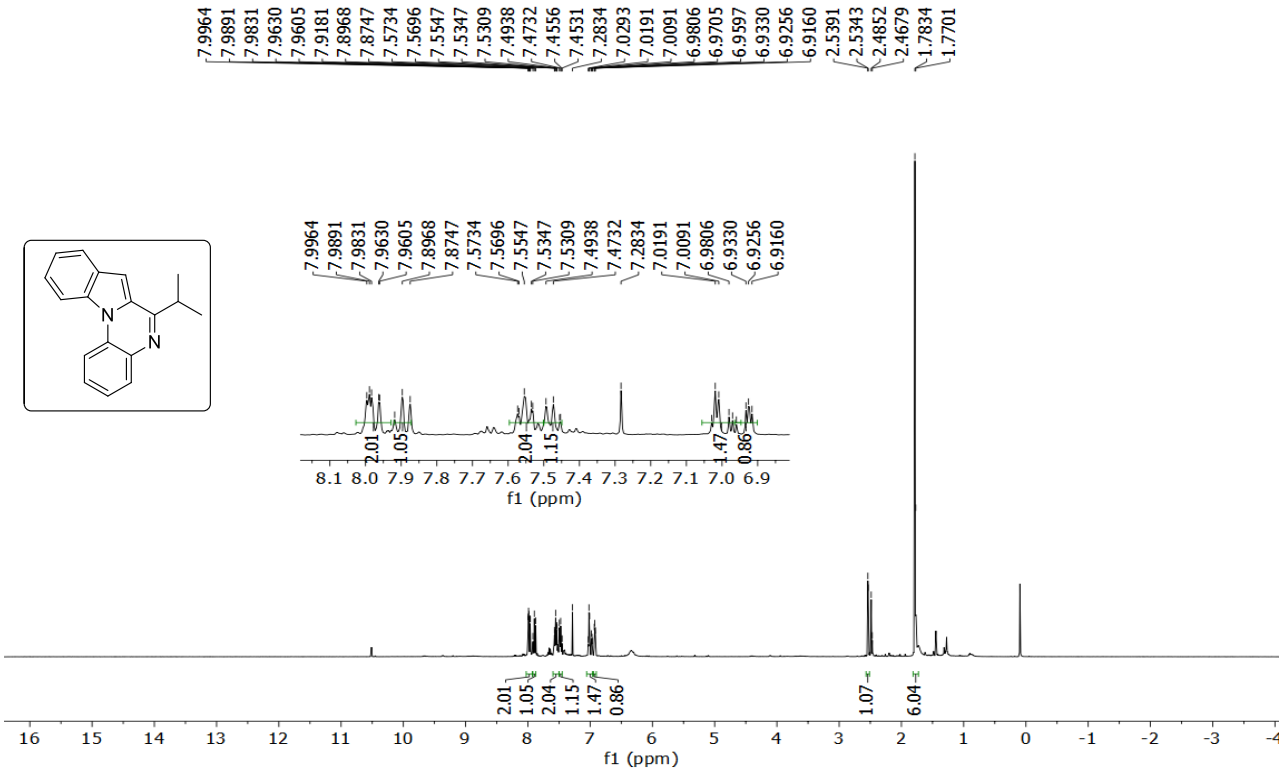


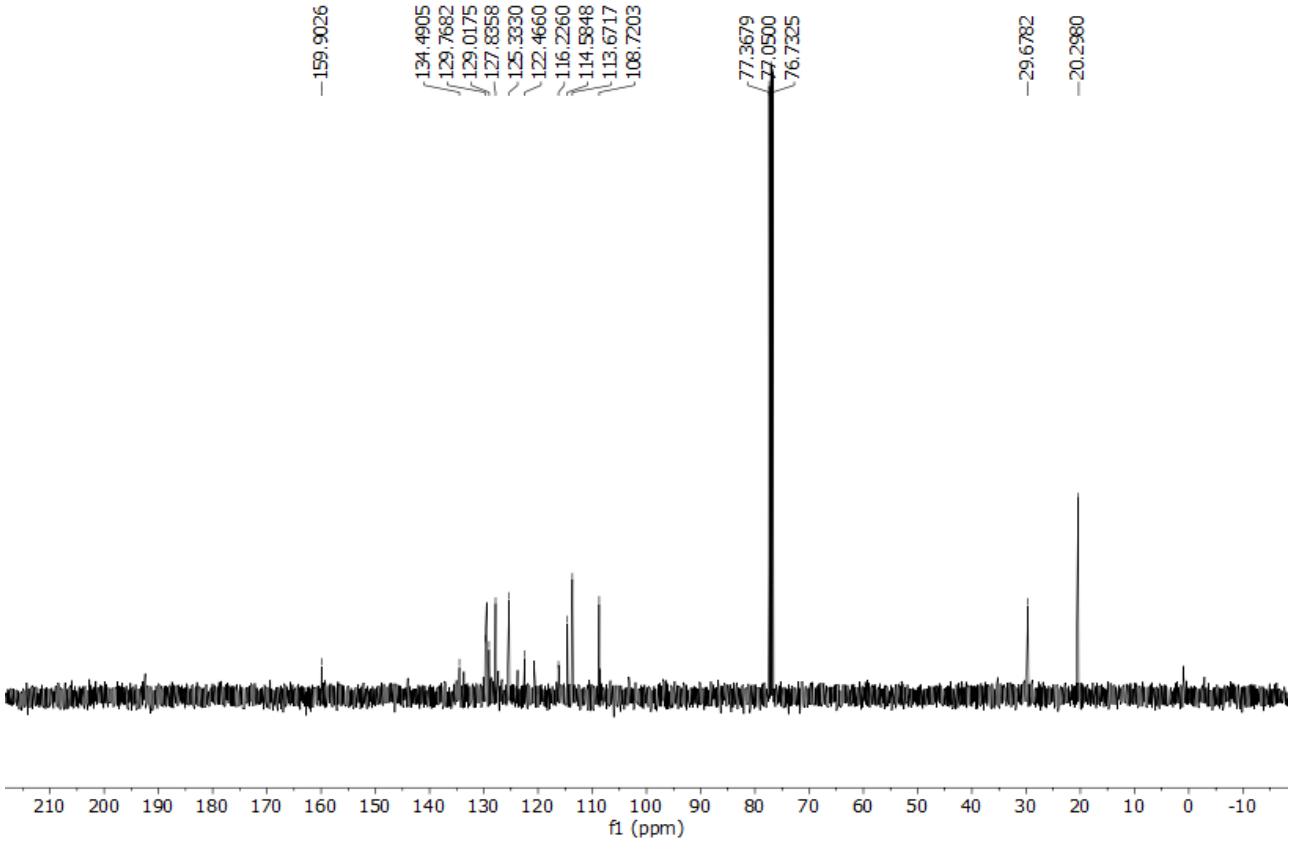

**6-isobutylindolo[1,2-*a*]quinoxaline (3d) :**

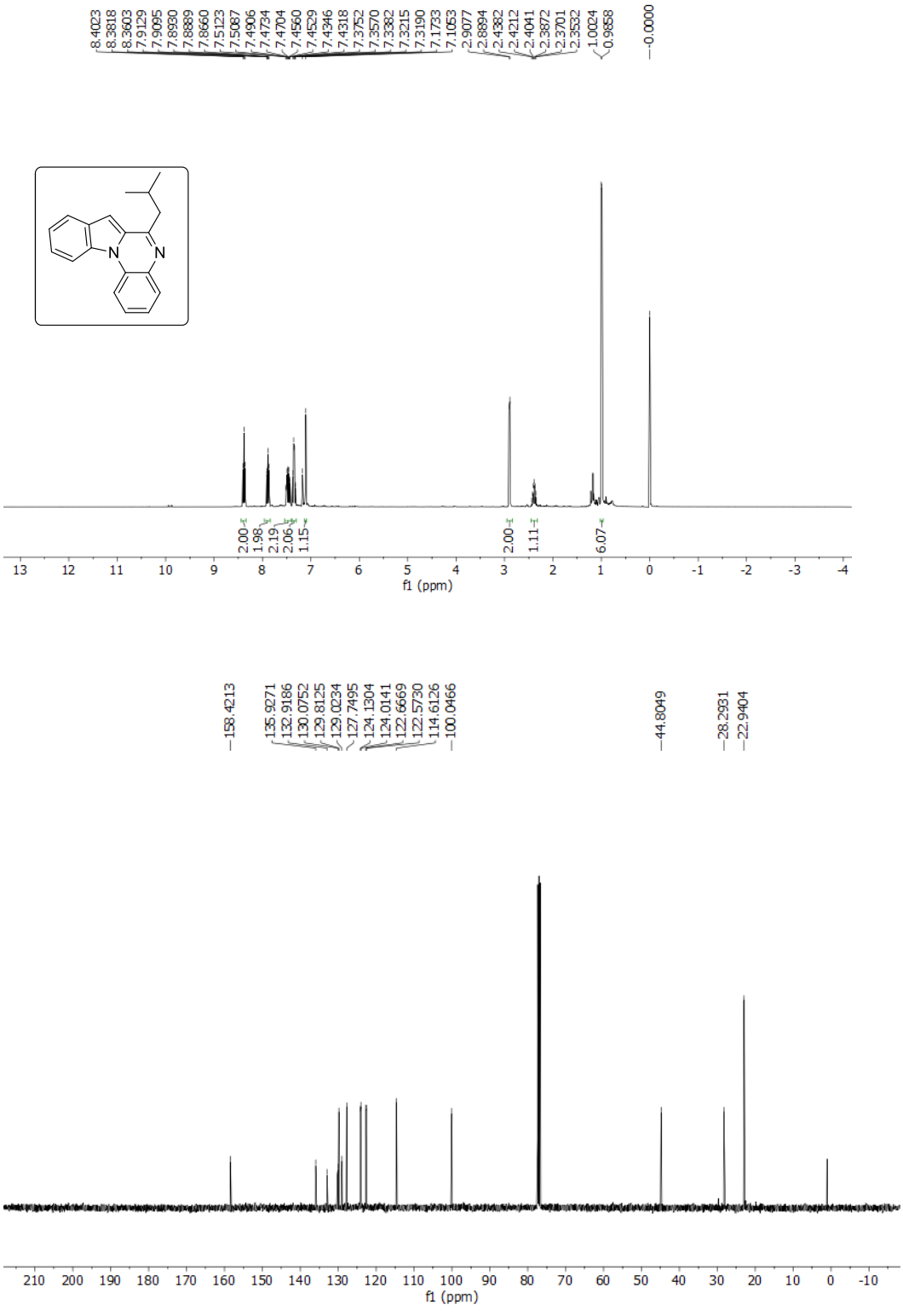

**6-phenylindolo[1,2-*a*]quinoxaline (3e) :**

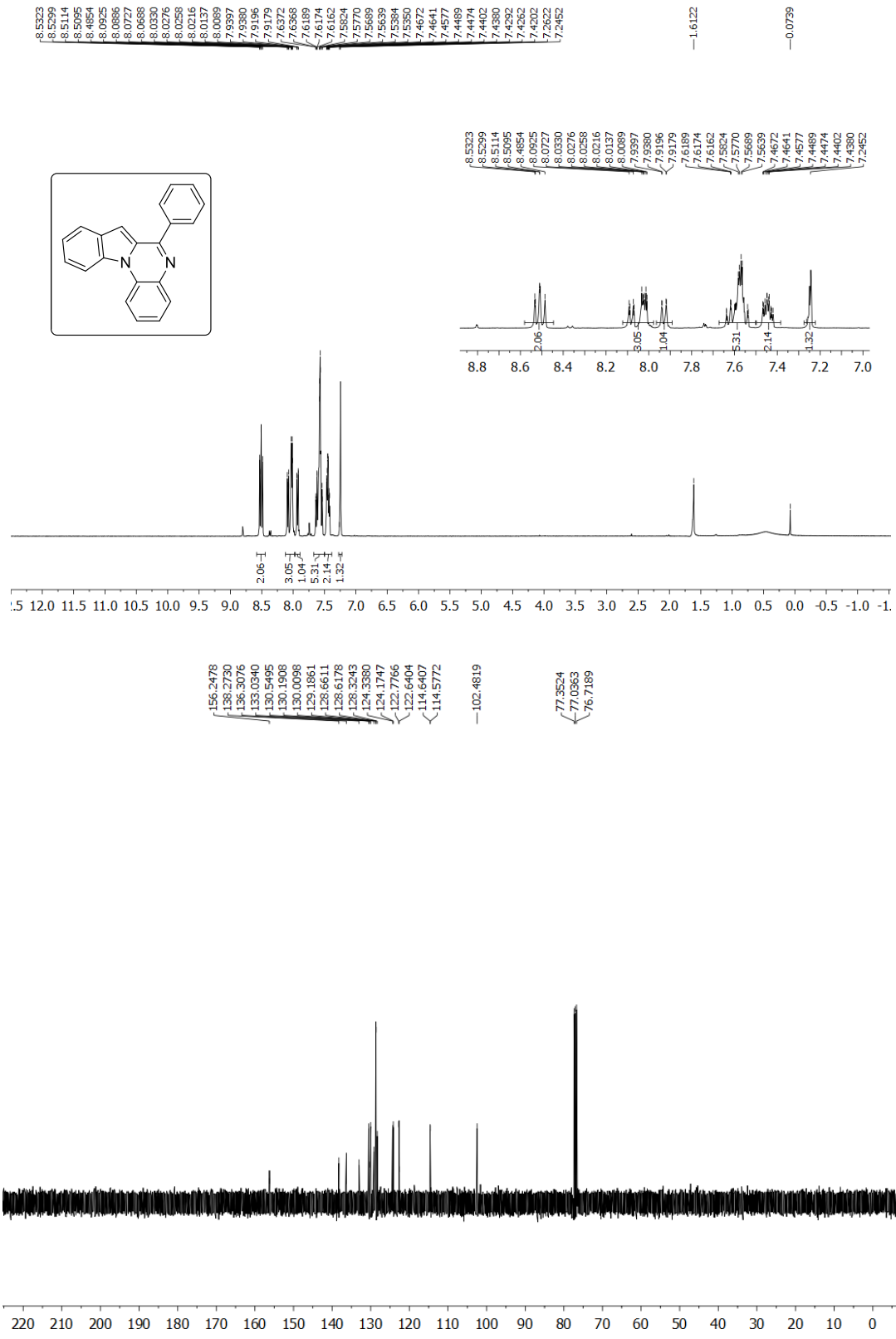

**6-(p-tolyl)indolo[1,2-*a*]quinoxaline (3f) :**

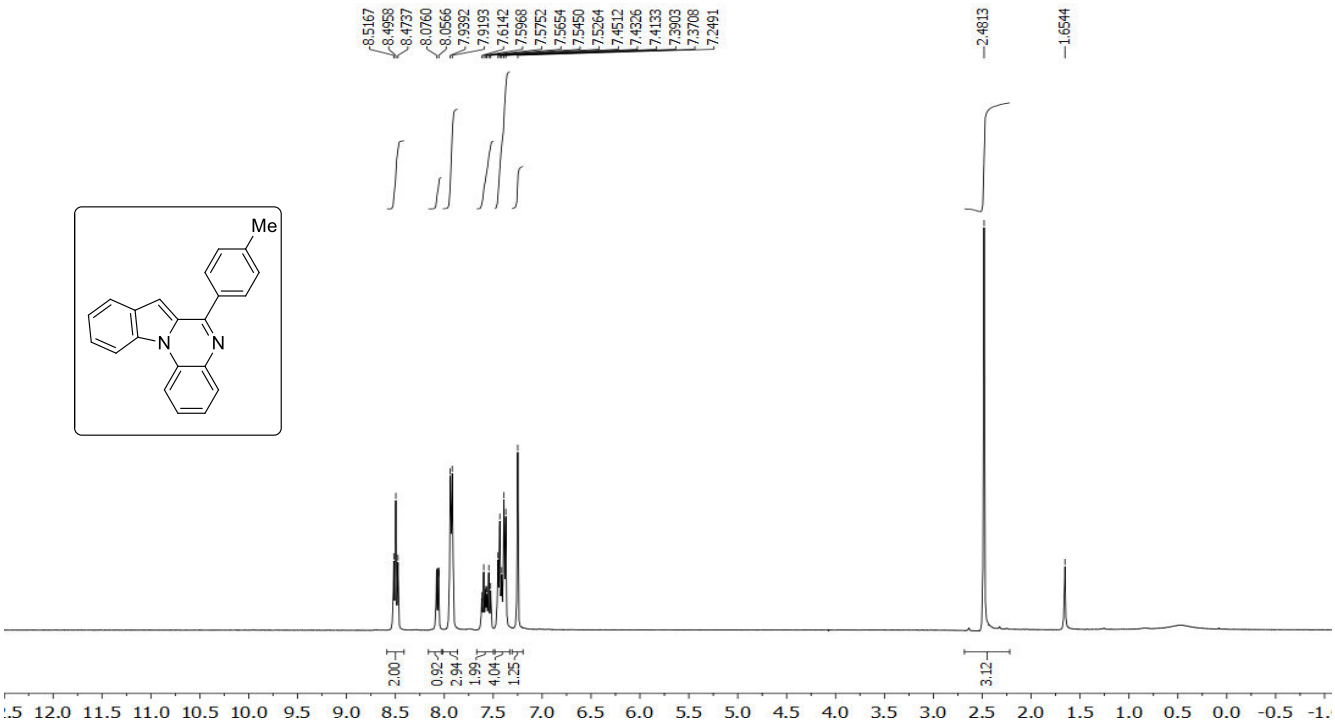


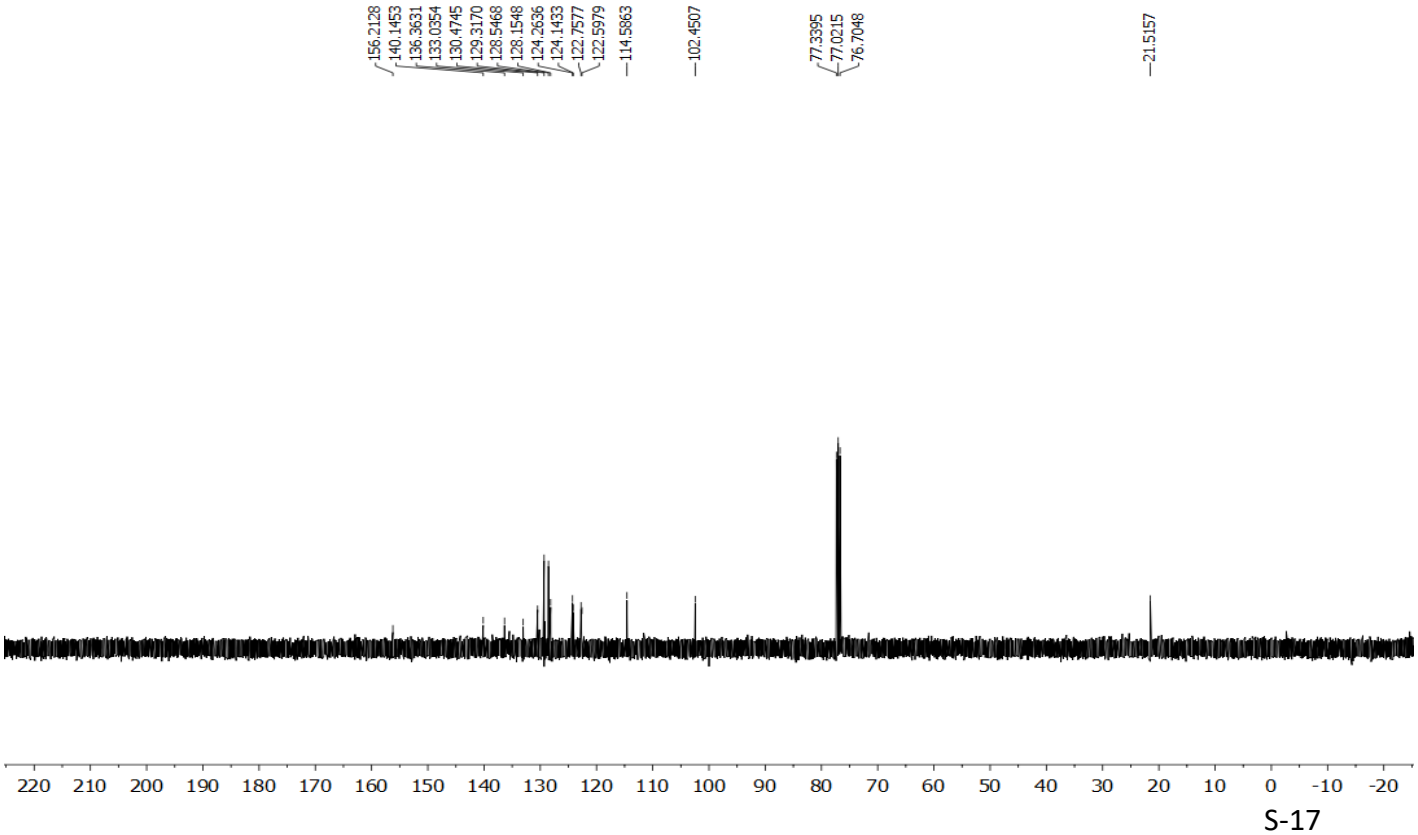

**6-(4-fluorophenyl)indolo[1,2-*a*]quinoxaline (3g) :**

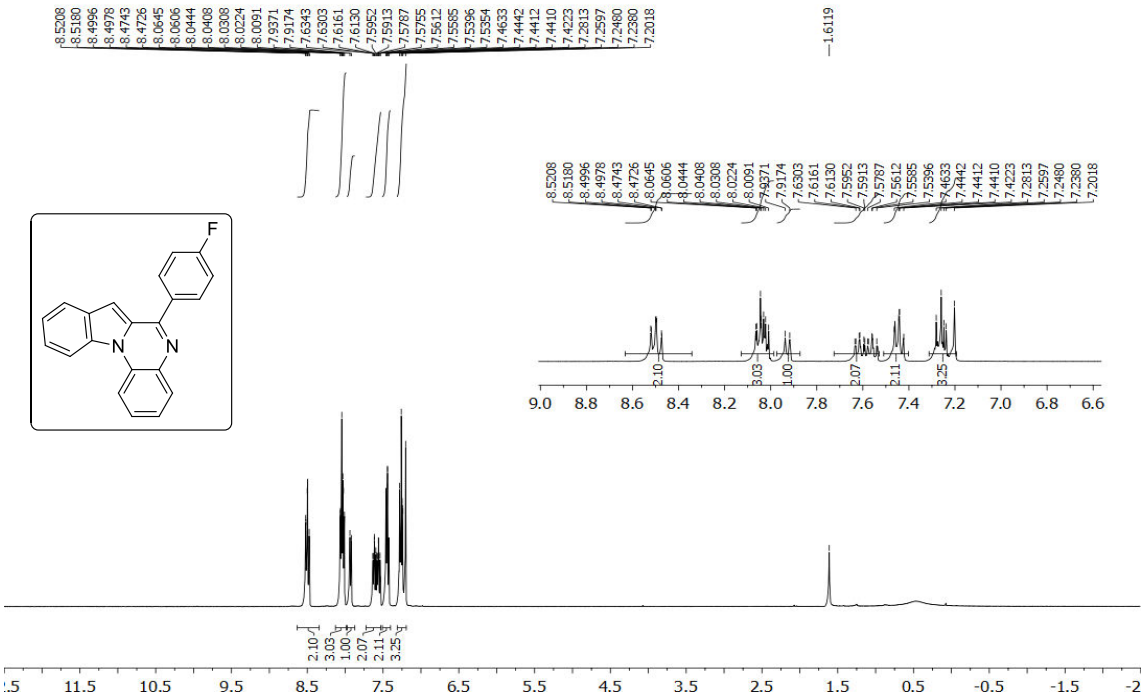


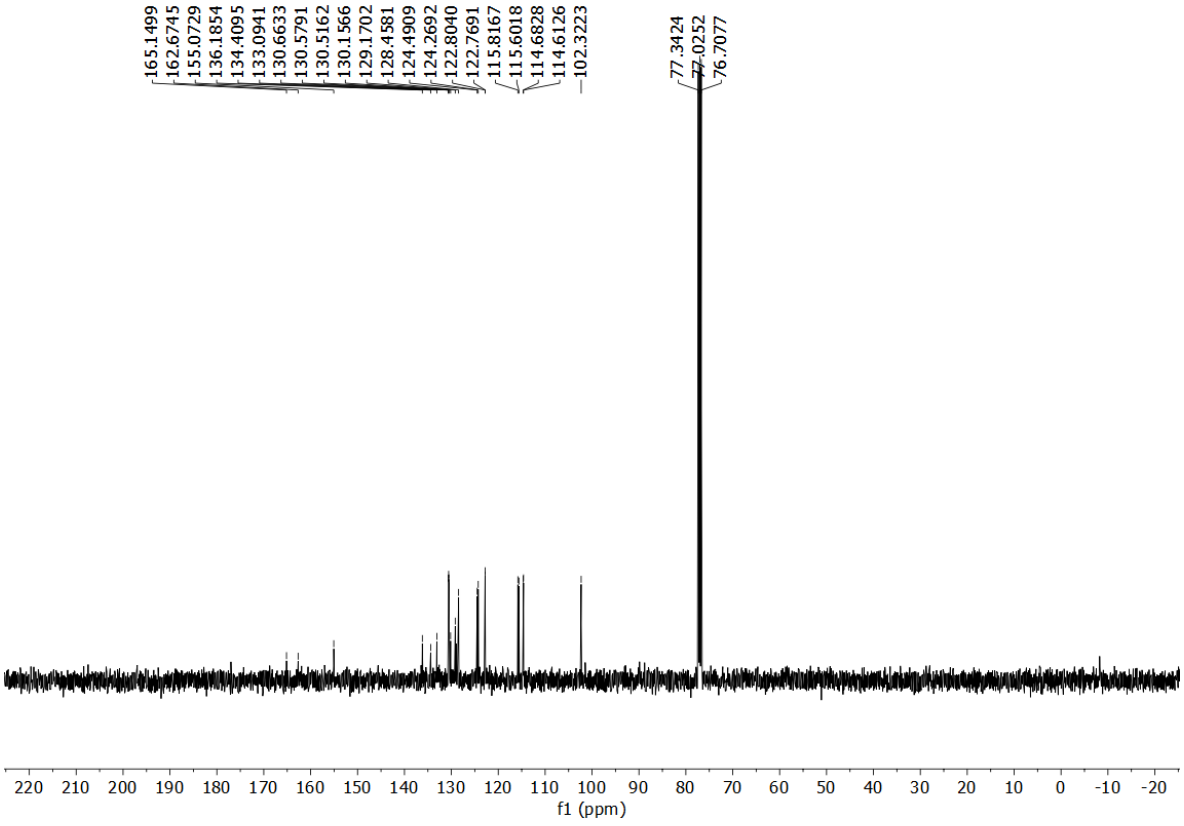

**6-(4-fluorophenyl)indolo[1,2-*a*]quinoxaline (3g) :**

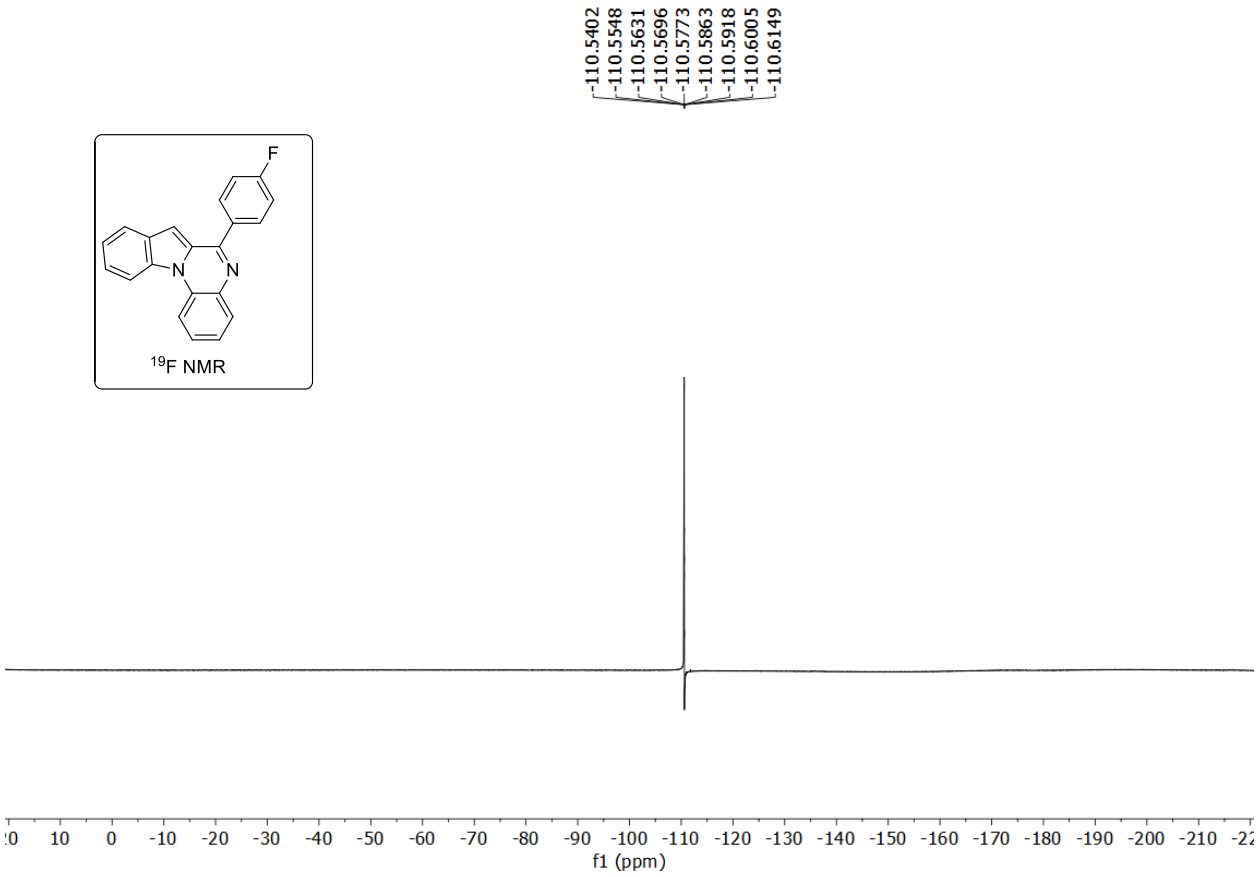

**6-(2-chlorophenyl)indolo[1,2-*a*]quinoxaline (3h) :**

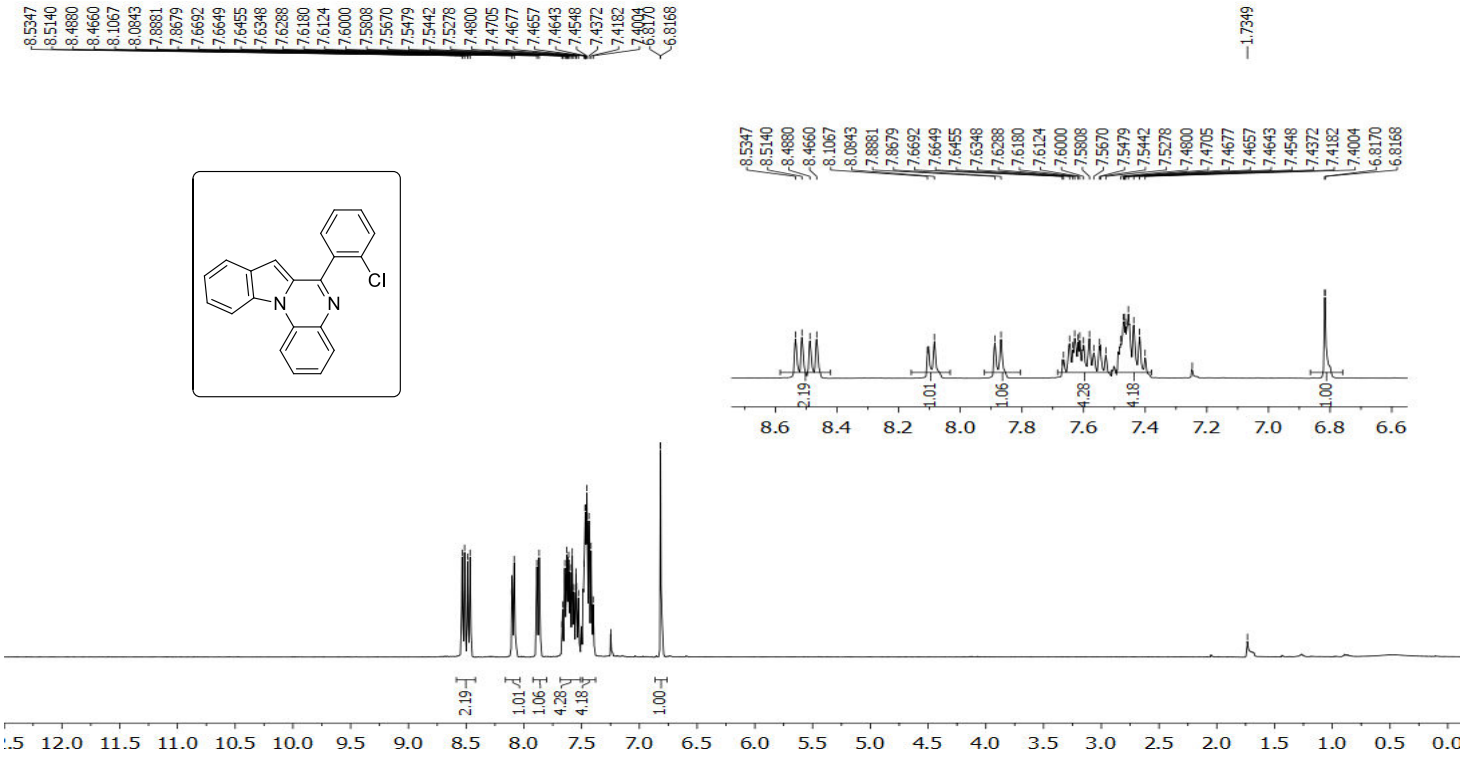


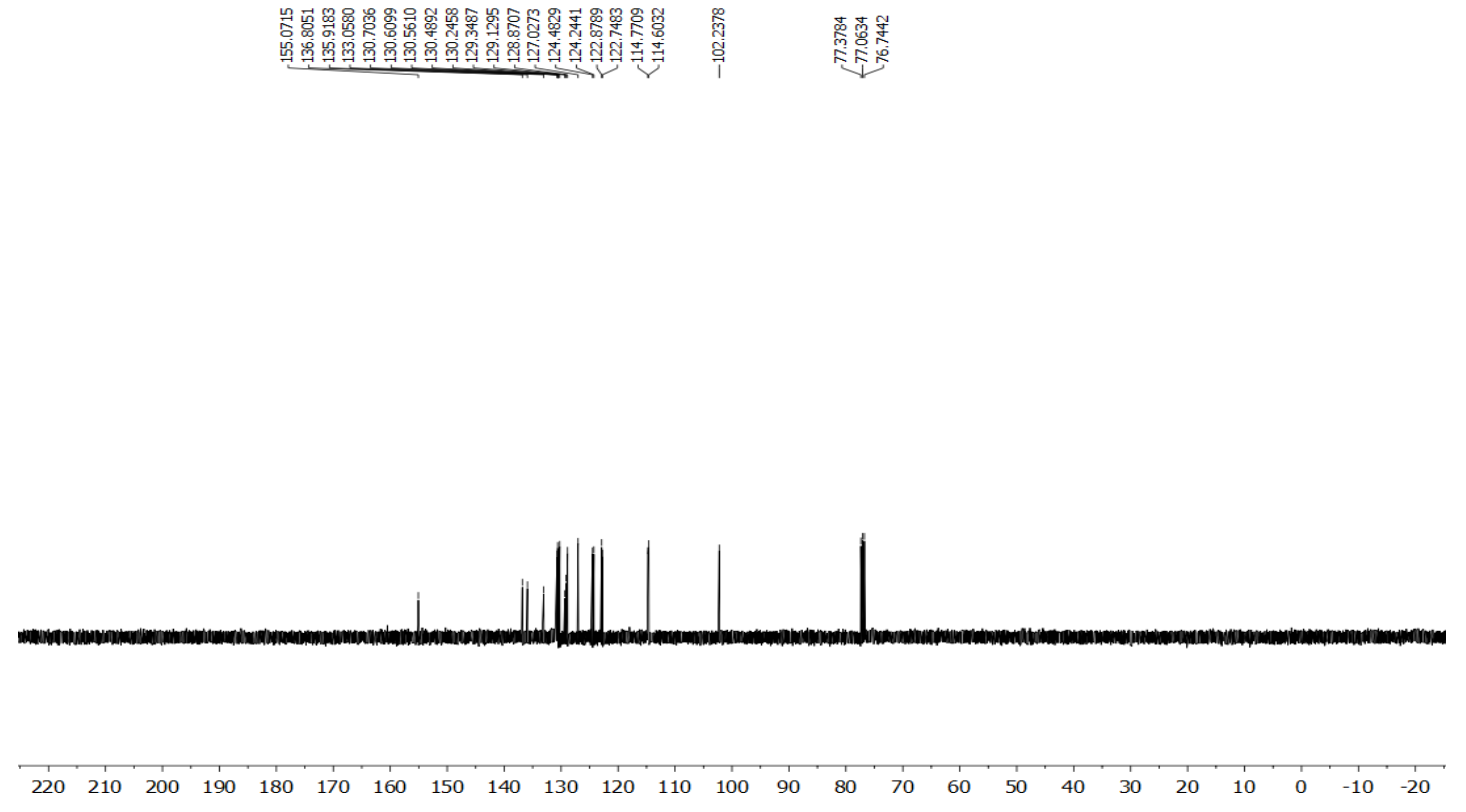

**9-bromo-6-phenylindolo[1,2-*a*]quinoxaline (3i) :**

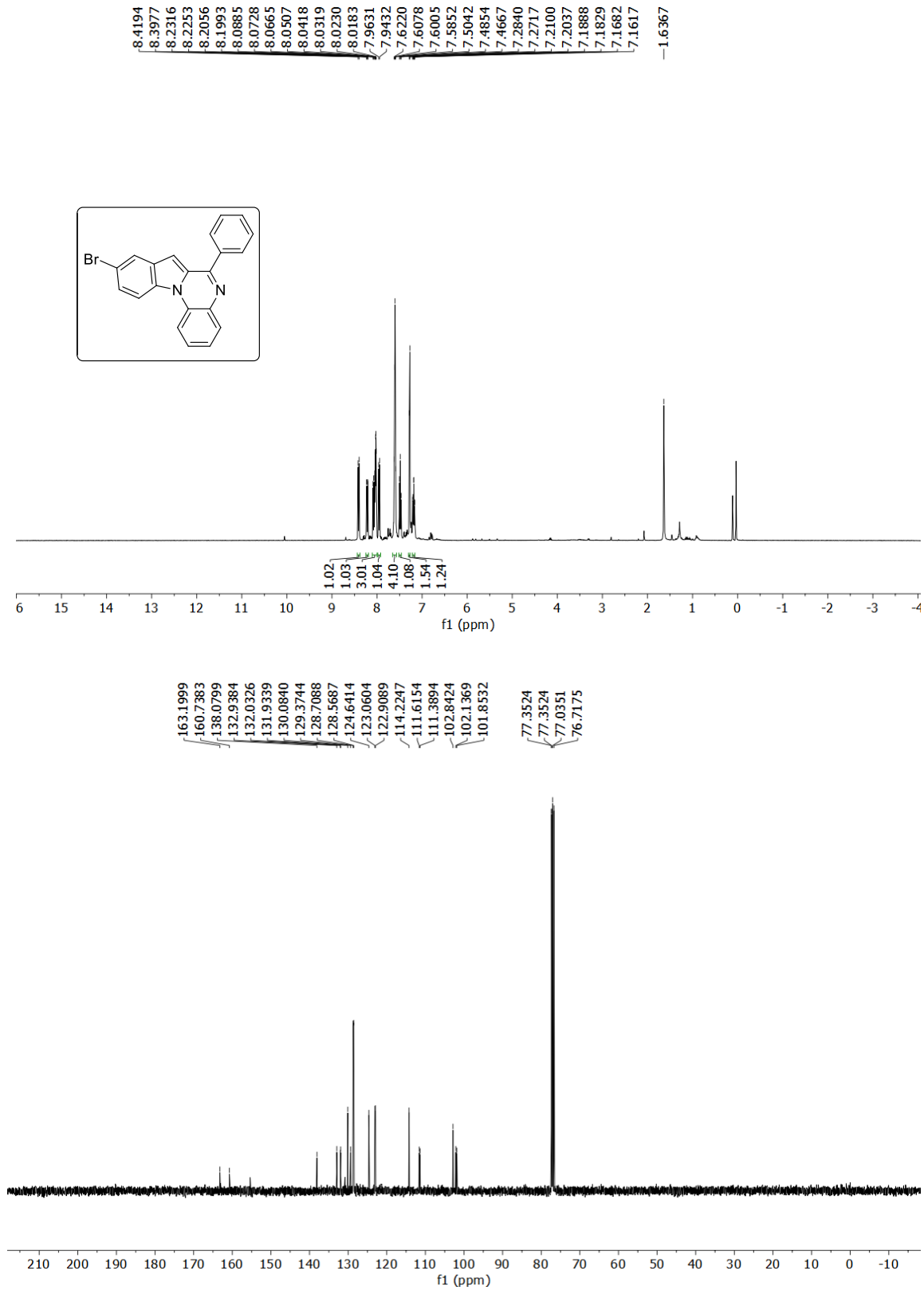

**3-fluoro-6-phenylindolo[1,2-*a*]quinoxaline (3j) :**

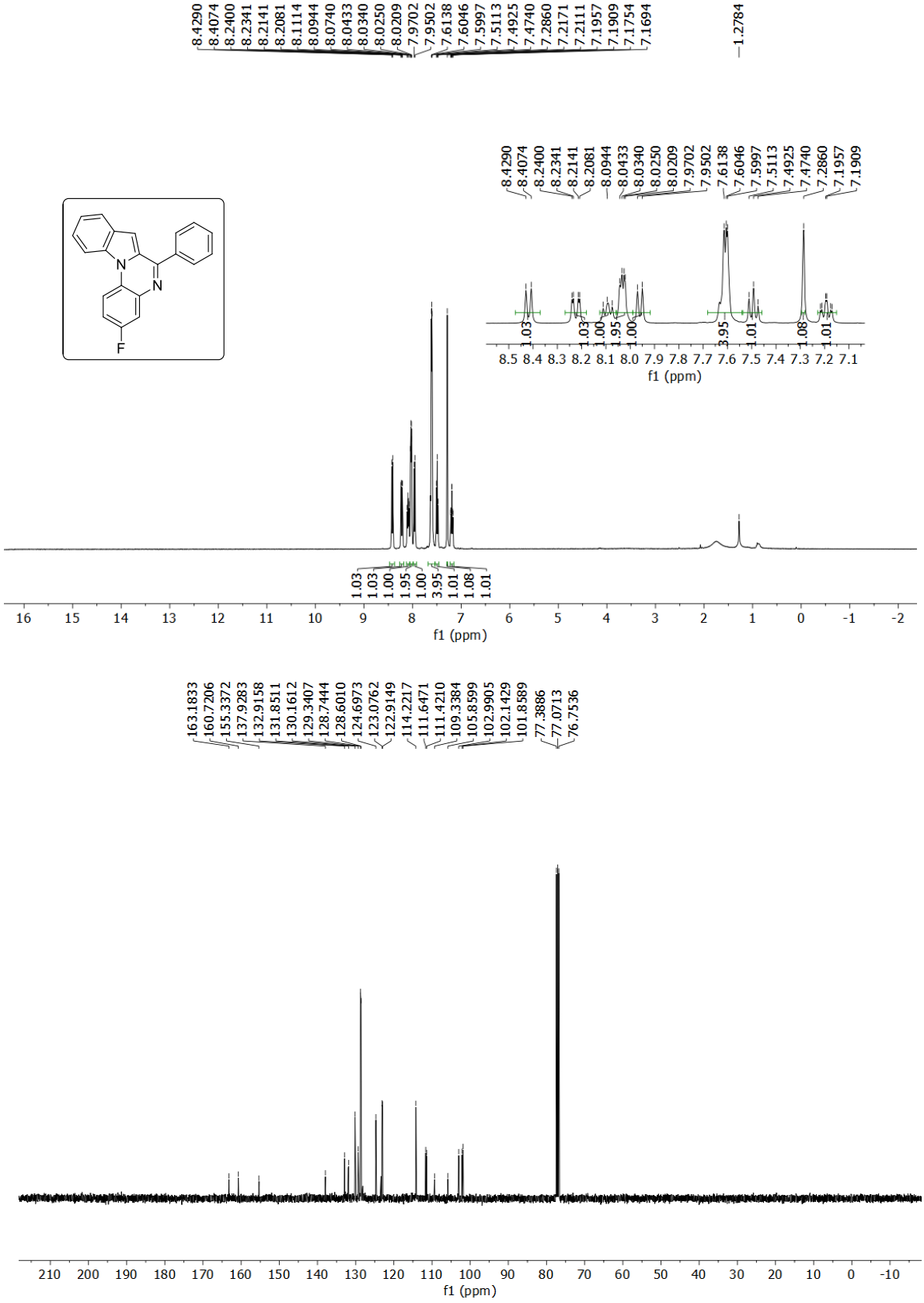

**3-fluoro-6-phenylindolo[1,2-*a*]quinoxaline (3j) :**

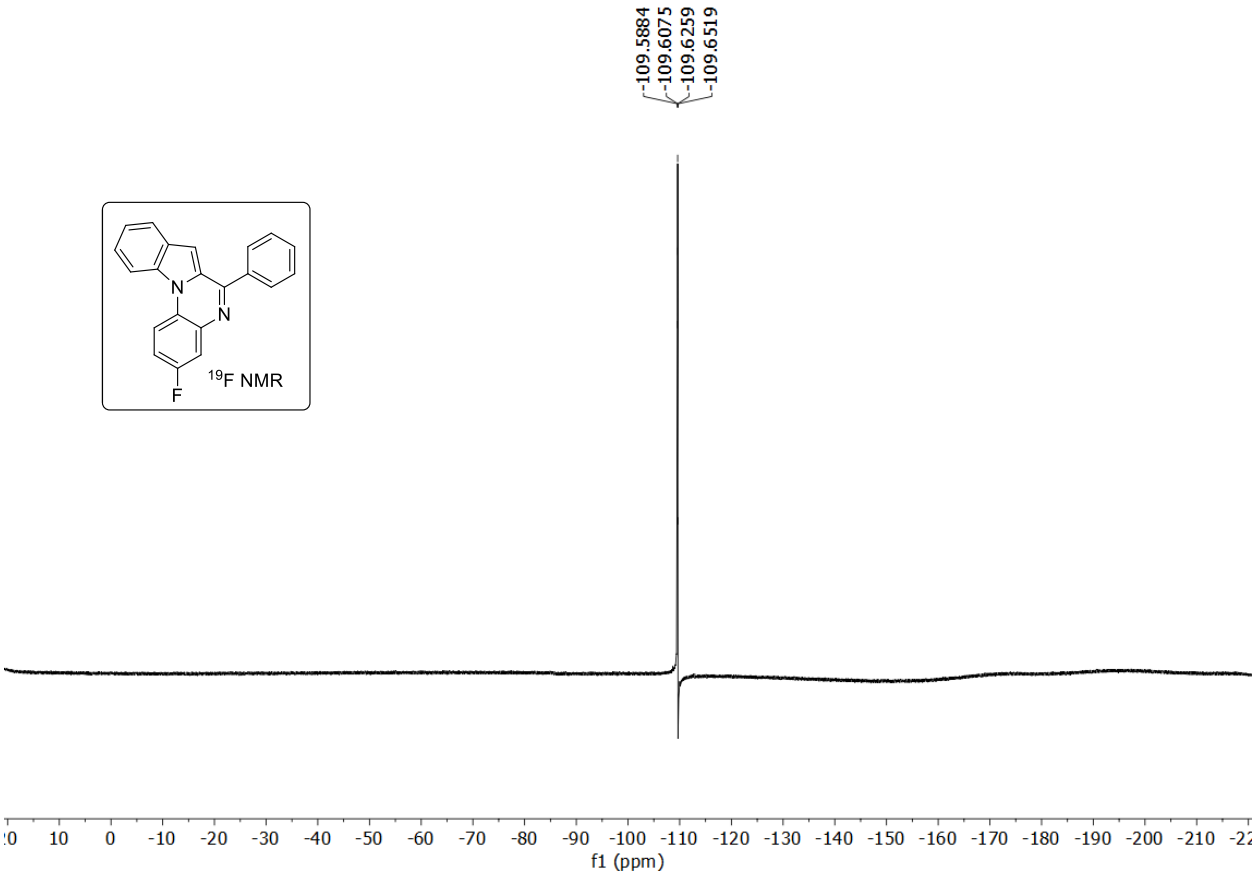

**(4-hydroxyphenyl)(indolo[1,2-*a*]quinoxalin-6-yl)methanone (3k) :**

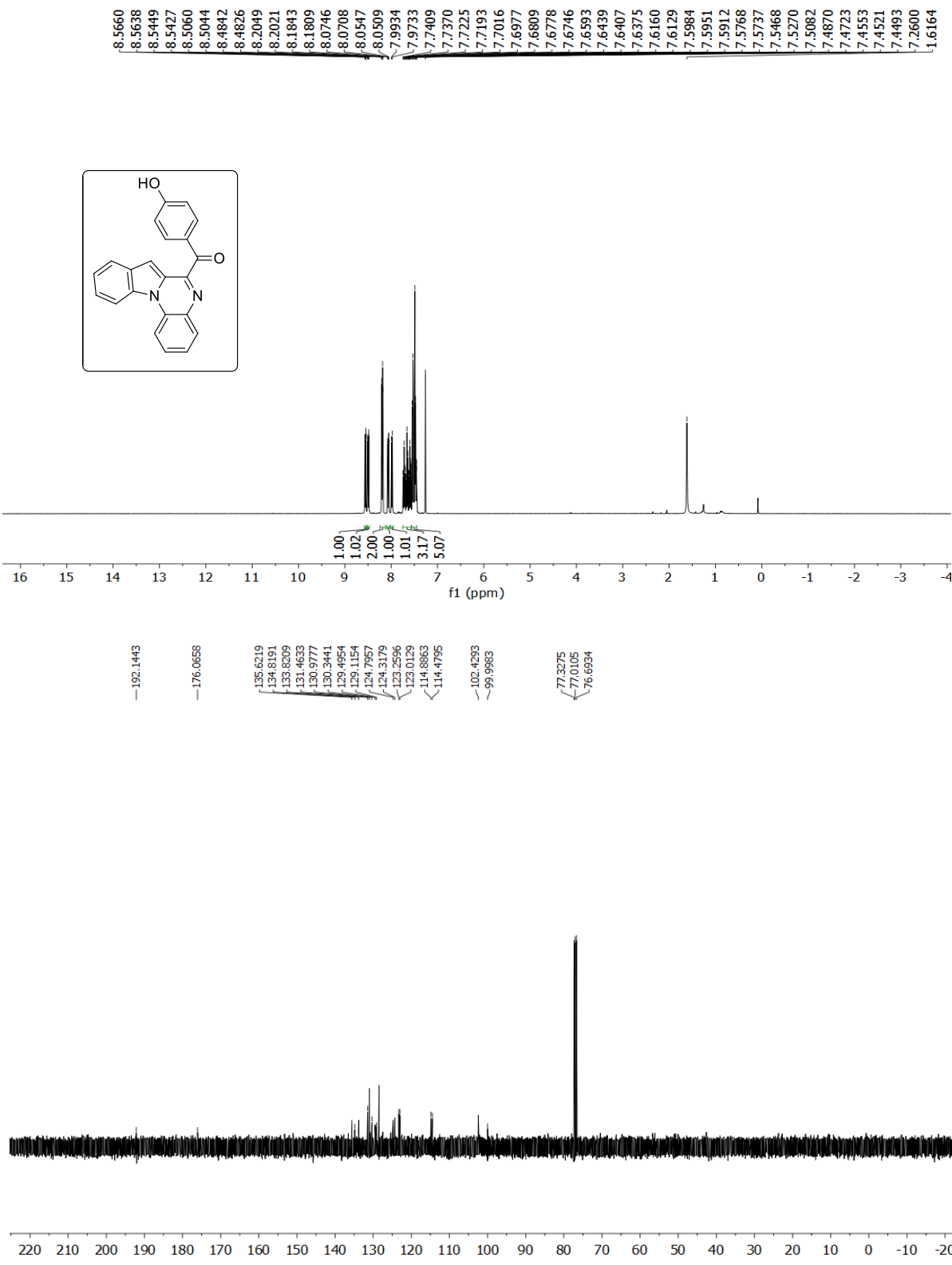

**Indolo[1,2-*α*]quinoxalin-6-yl(phenyl)methanone (3l) :**

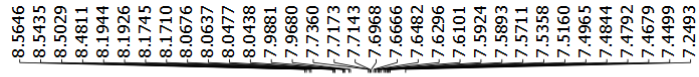


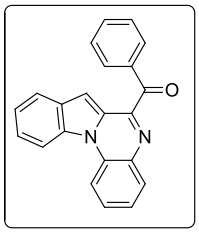


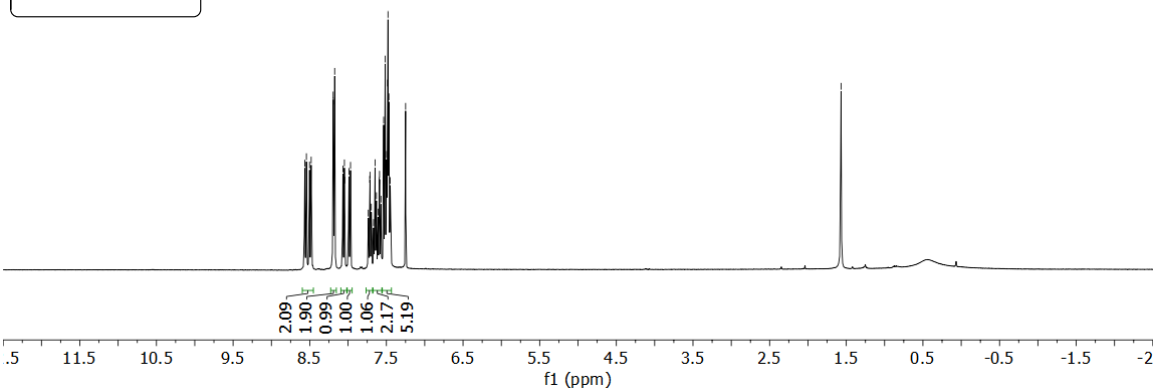


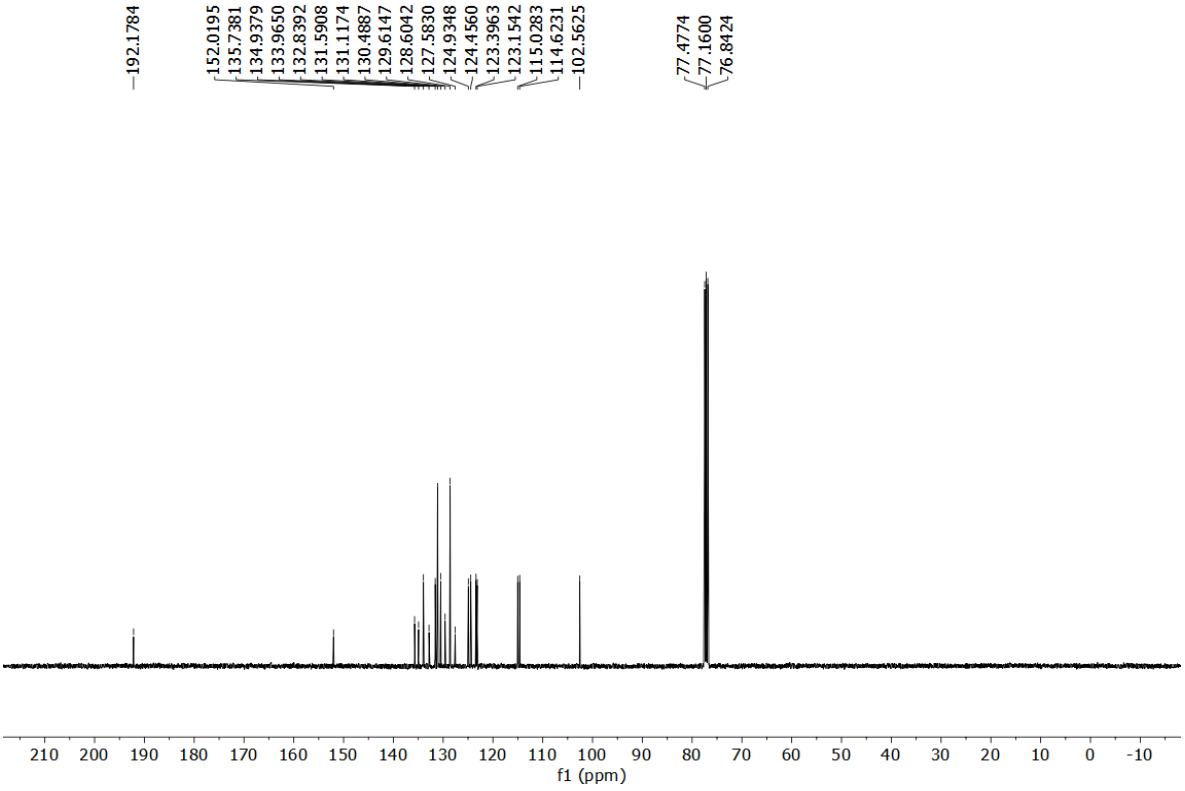

**Pyrrolo[1,2-*a*]quinoxaline (4a) :**

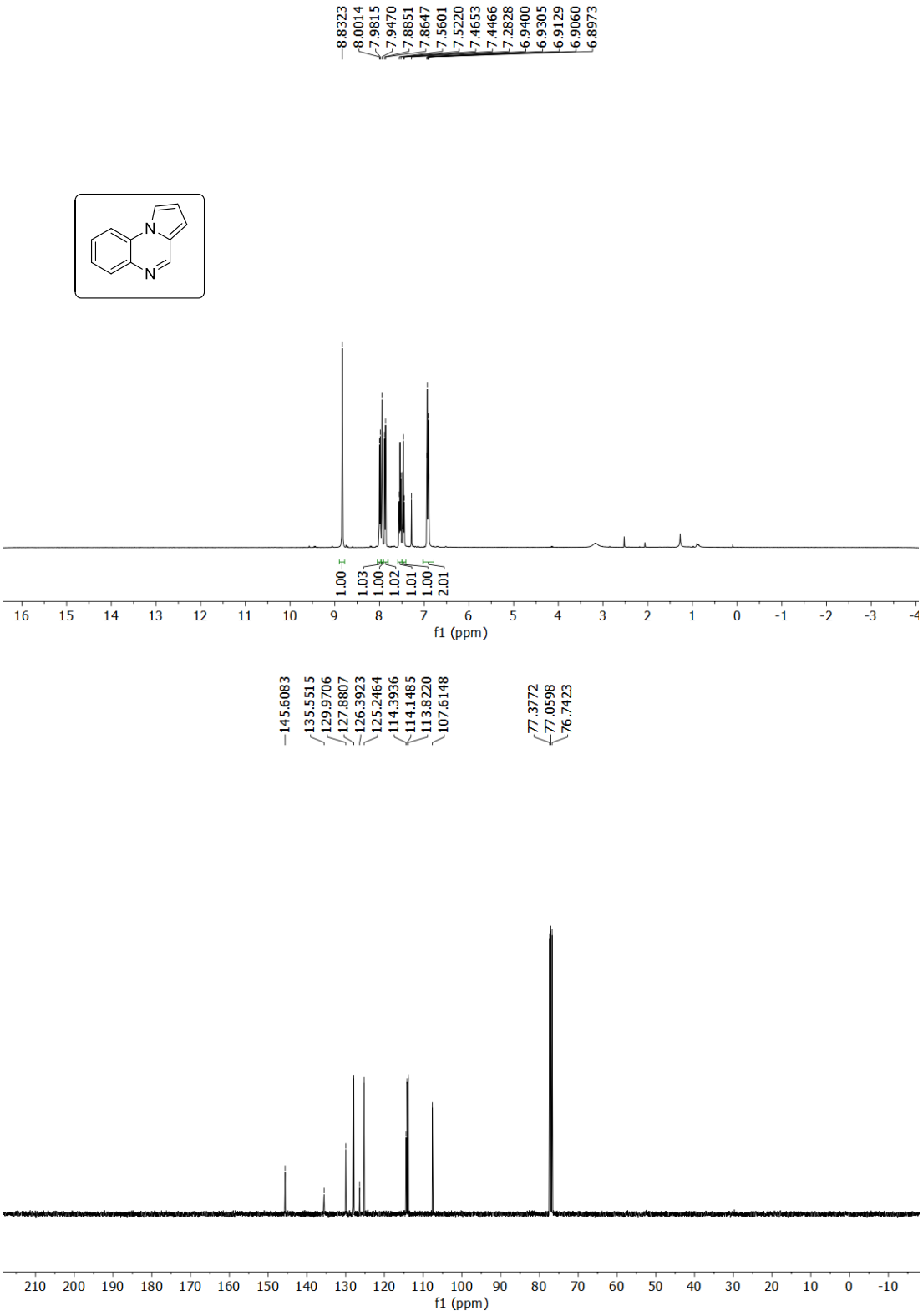

**4-methylpyrrolo[1,2-*a*]quinoxaline (4b) :**

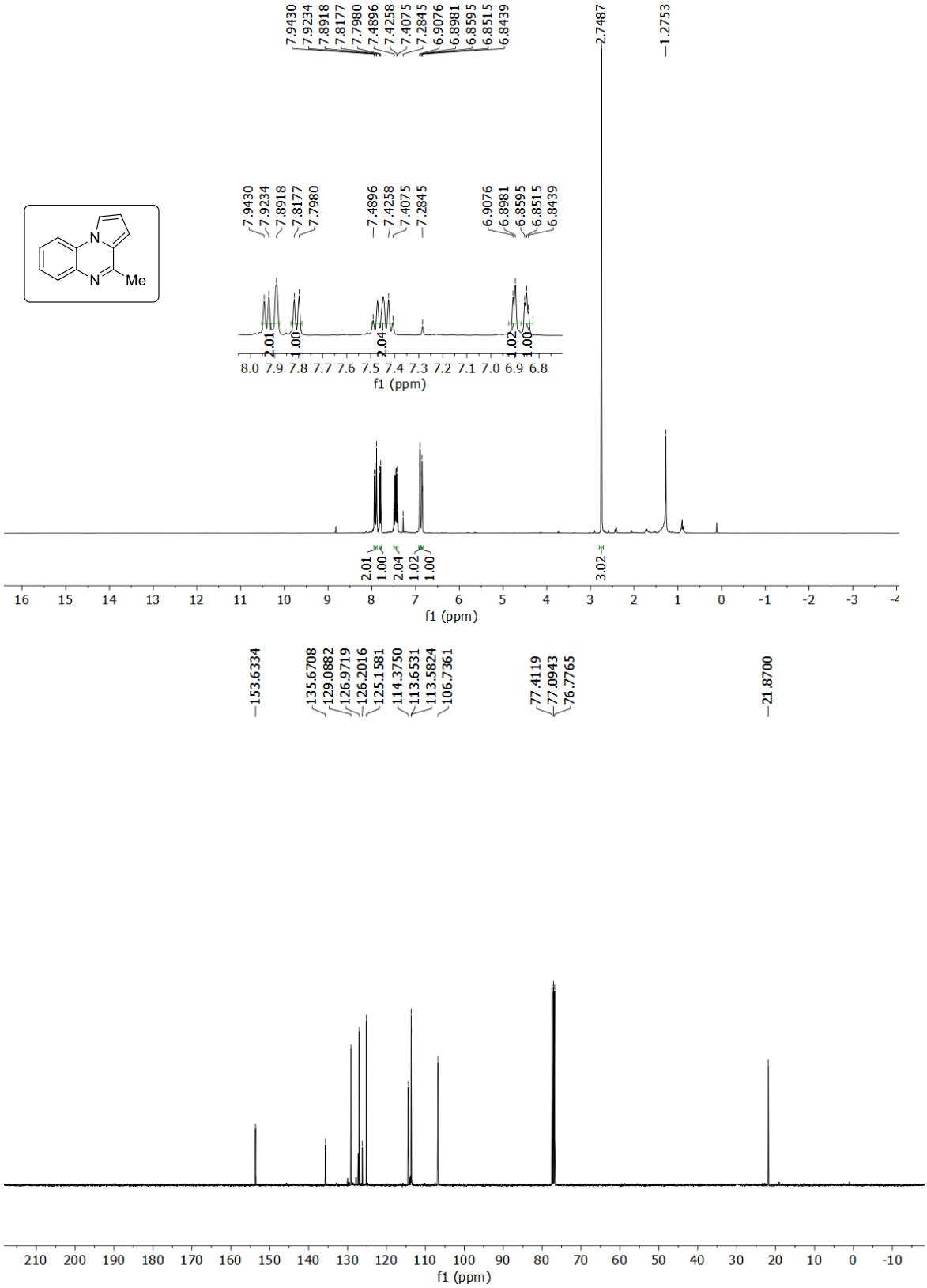

**4-isopropylpyrrolo[1,2-*a*]quinoxaline (4c) :**

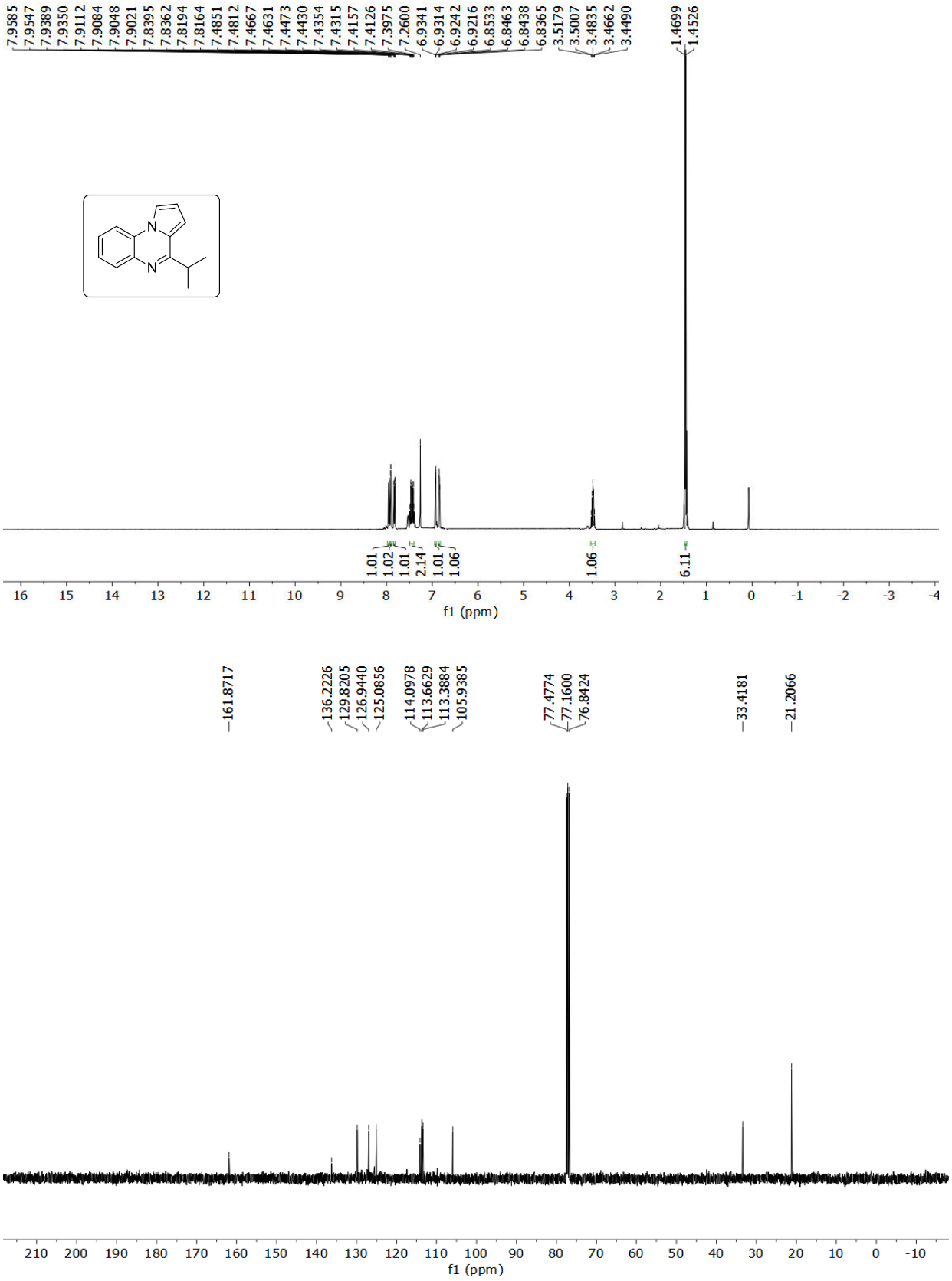

**4-phenylpyrrolo[1,2-*a*]quinoxaline (4d) :**

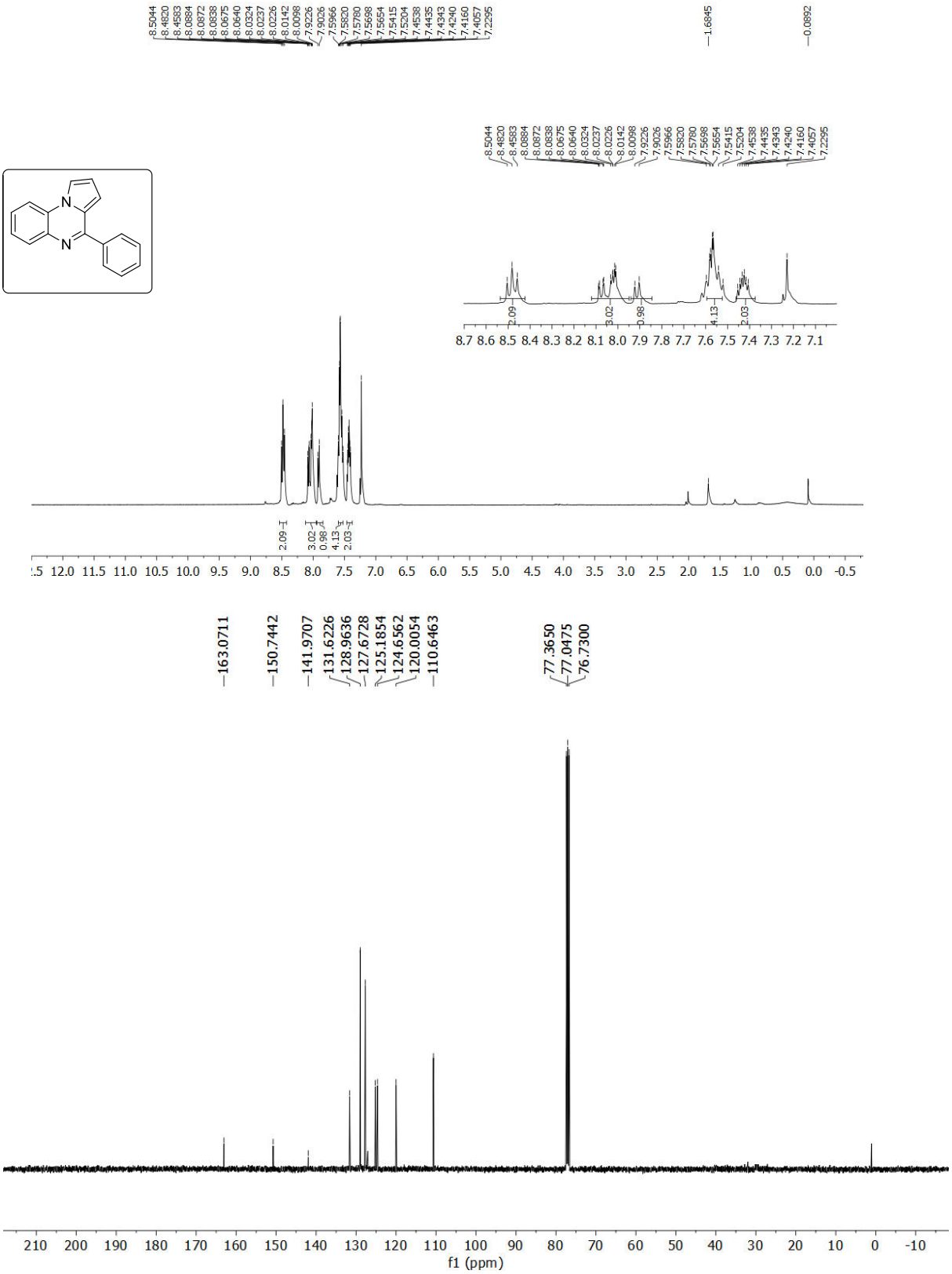

**4-(4-fluorophenyl)pyrrolo[1,2-*a*]quinoxaline (4e) :**

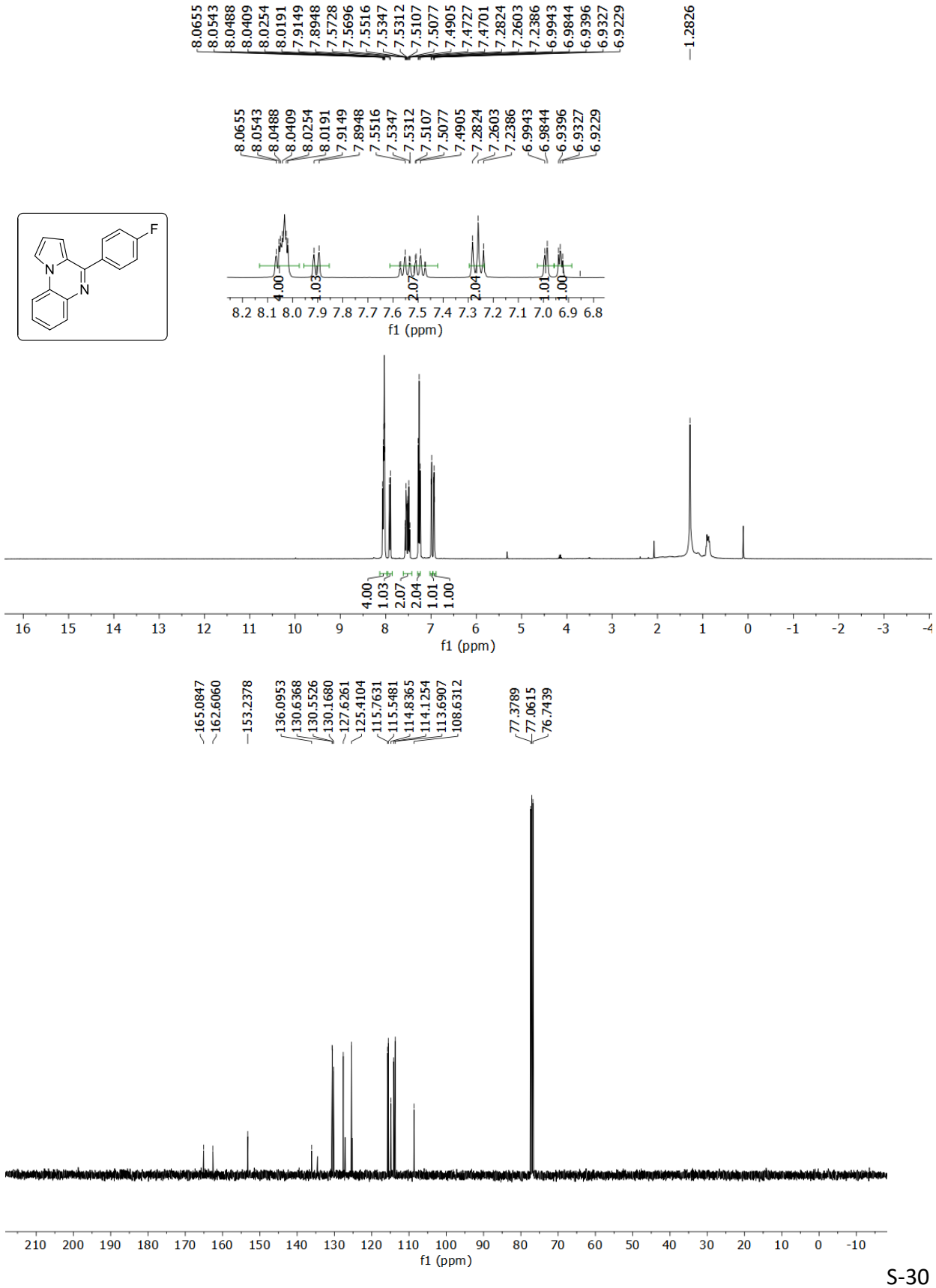

**4-(4-fluorophenyl)pyrrolo[1,2-*a*]quinoxaline (4e) :**

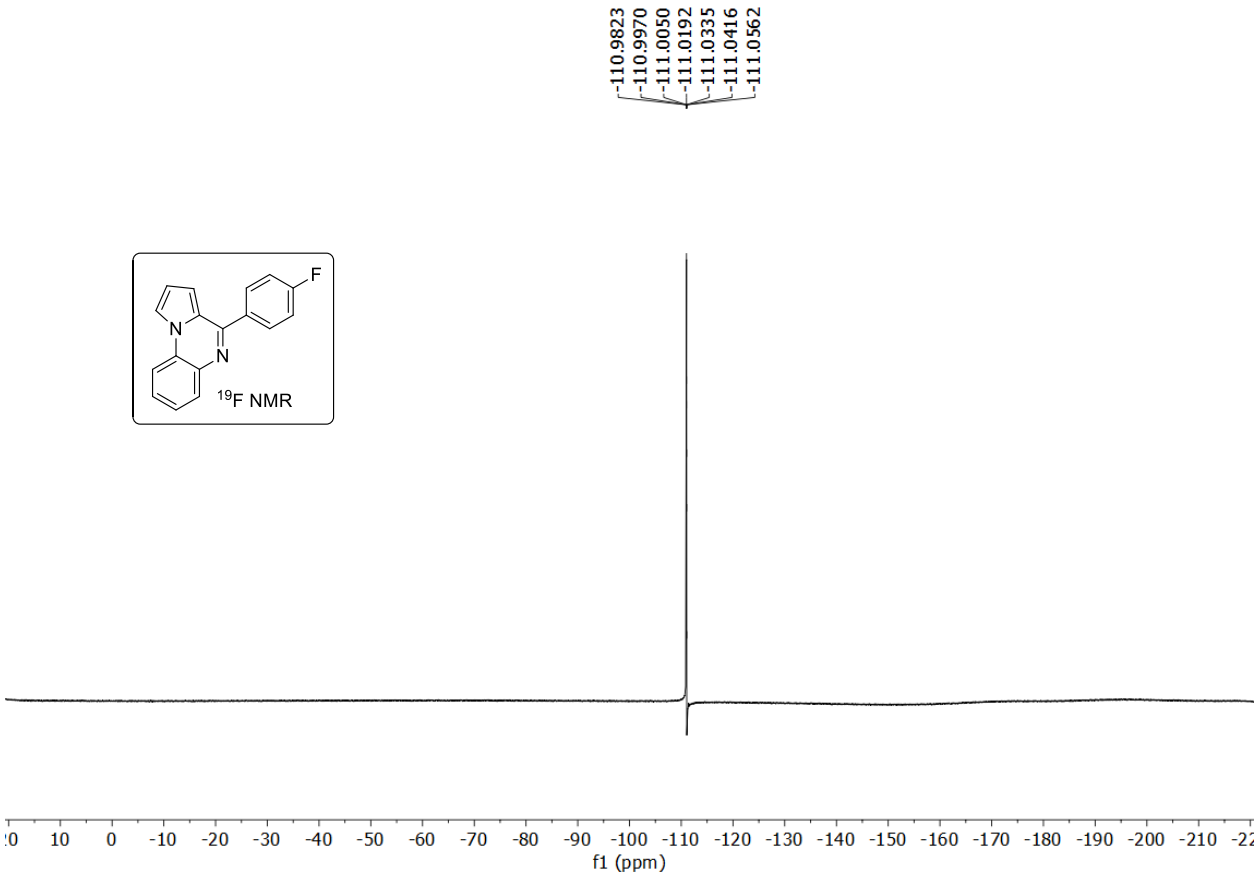

**4-(2-chlorophenyl)pyrrolo[1,2-*a*]quinoxaline (4f) :**

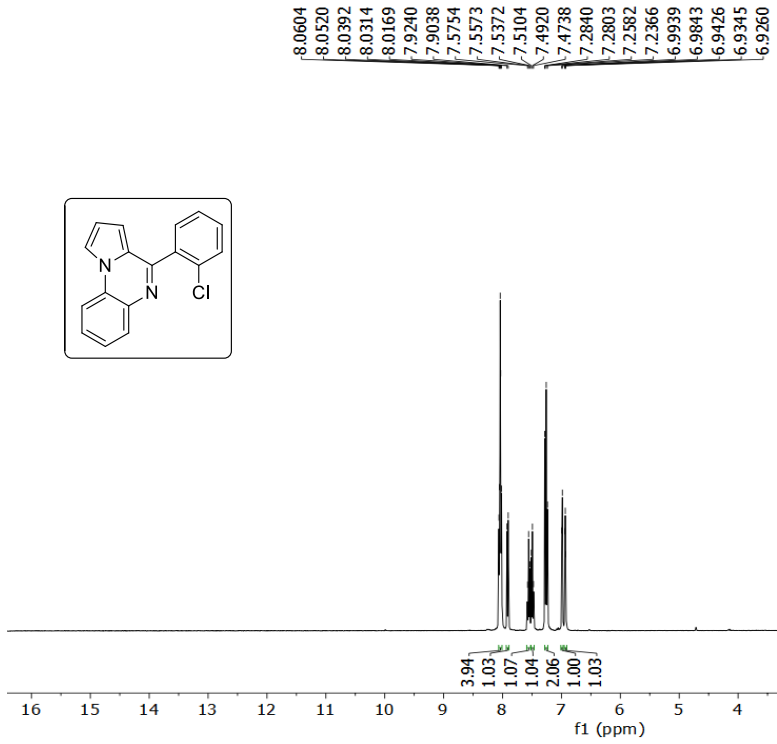


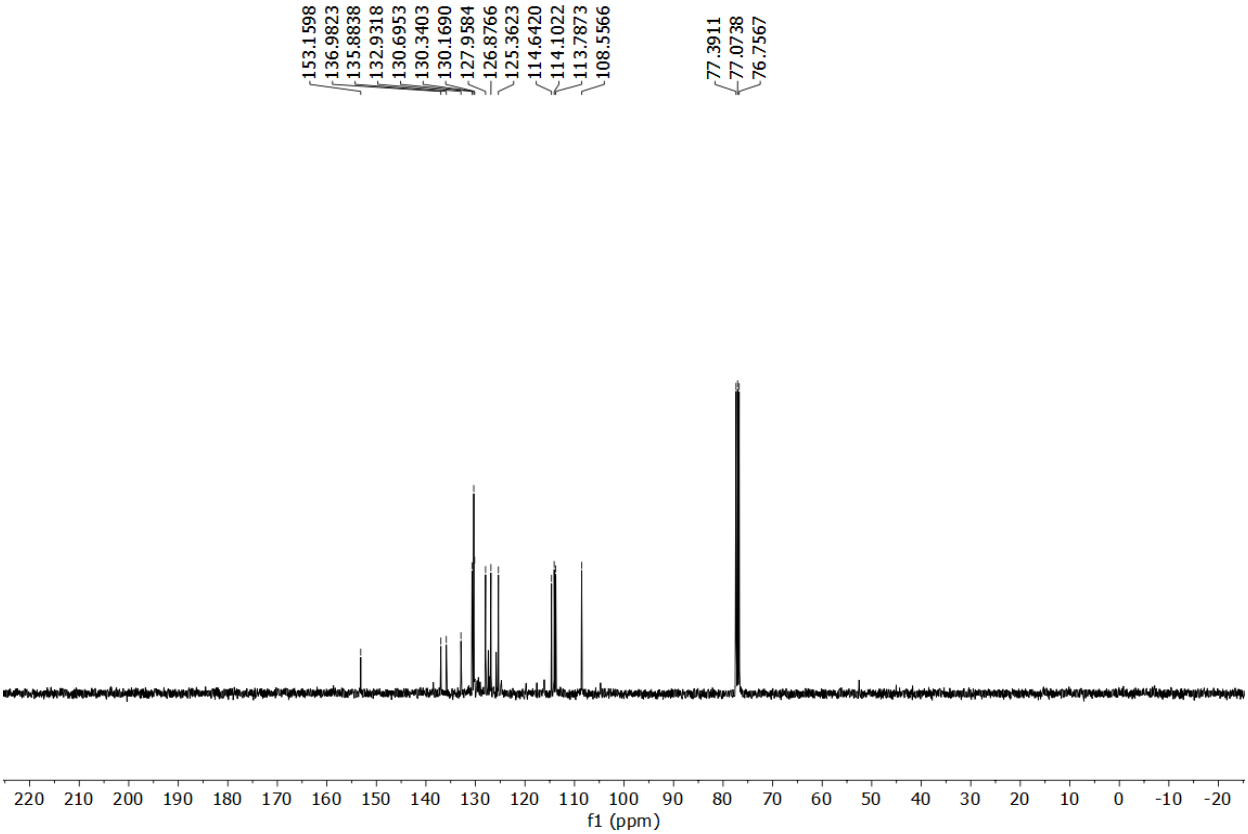

**7-methyl-4-phenylpyrrolo[1,2-*a*]quinoxaline (4g) :**

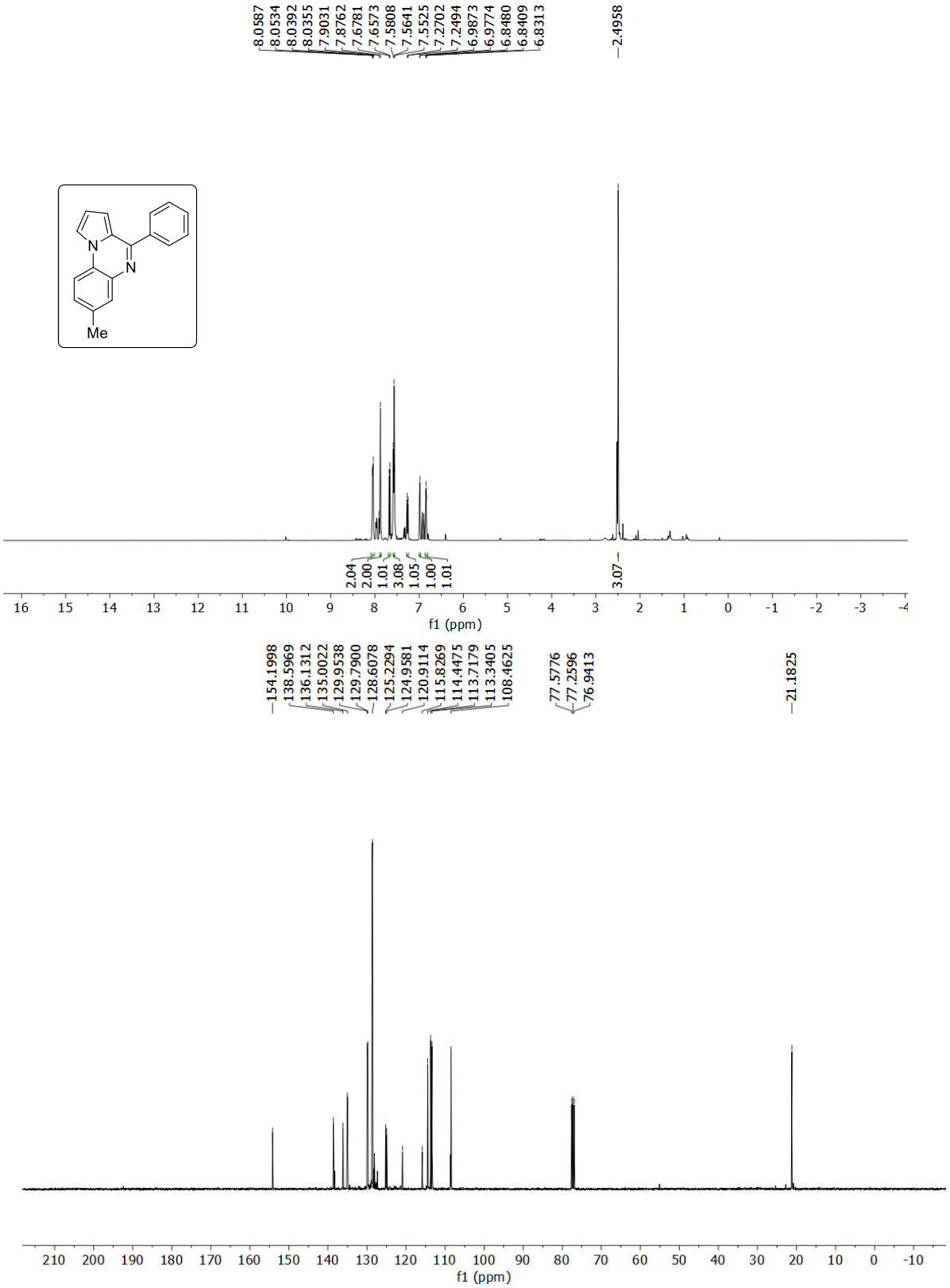

**7-methoxy-4-phenylpyrrolo[1,2-*a*]quinoxaline (4h) :**

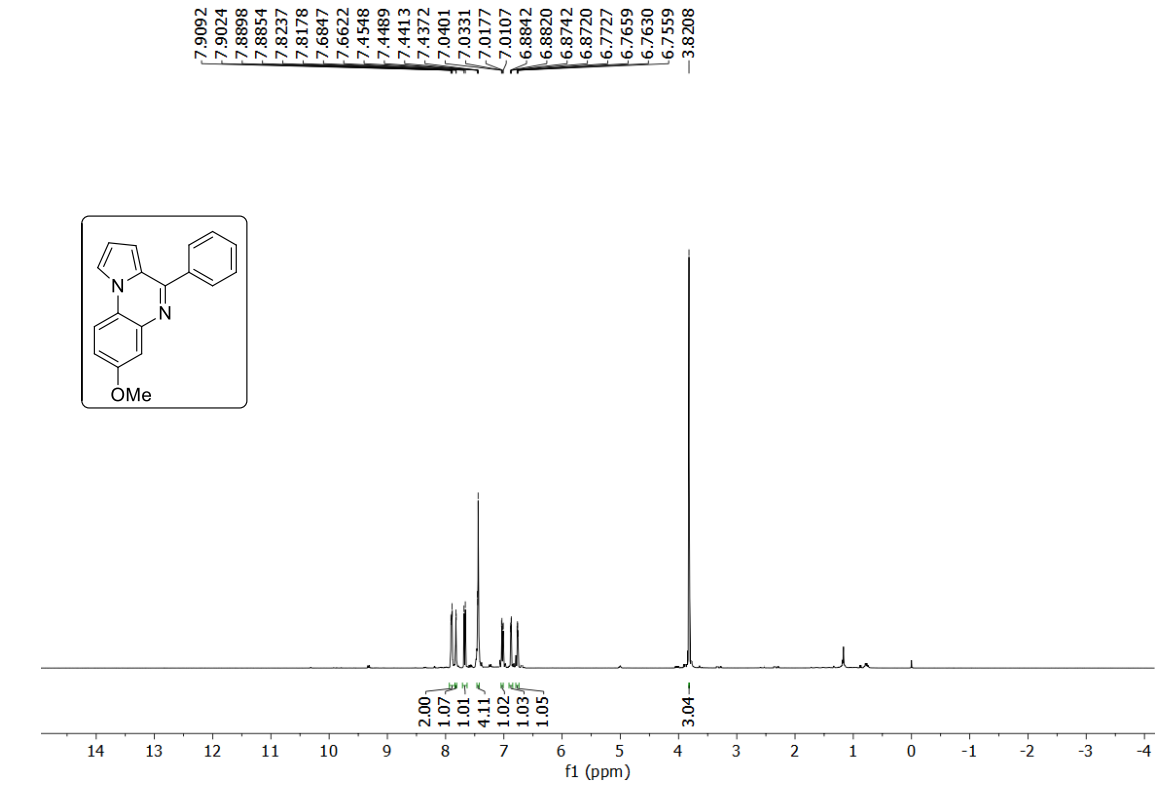


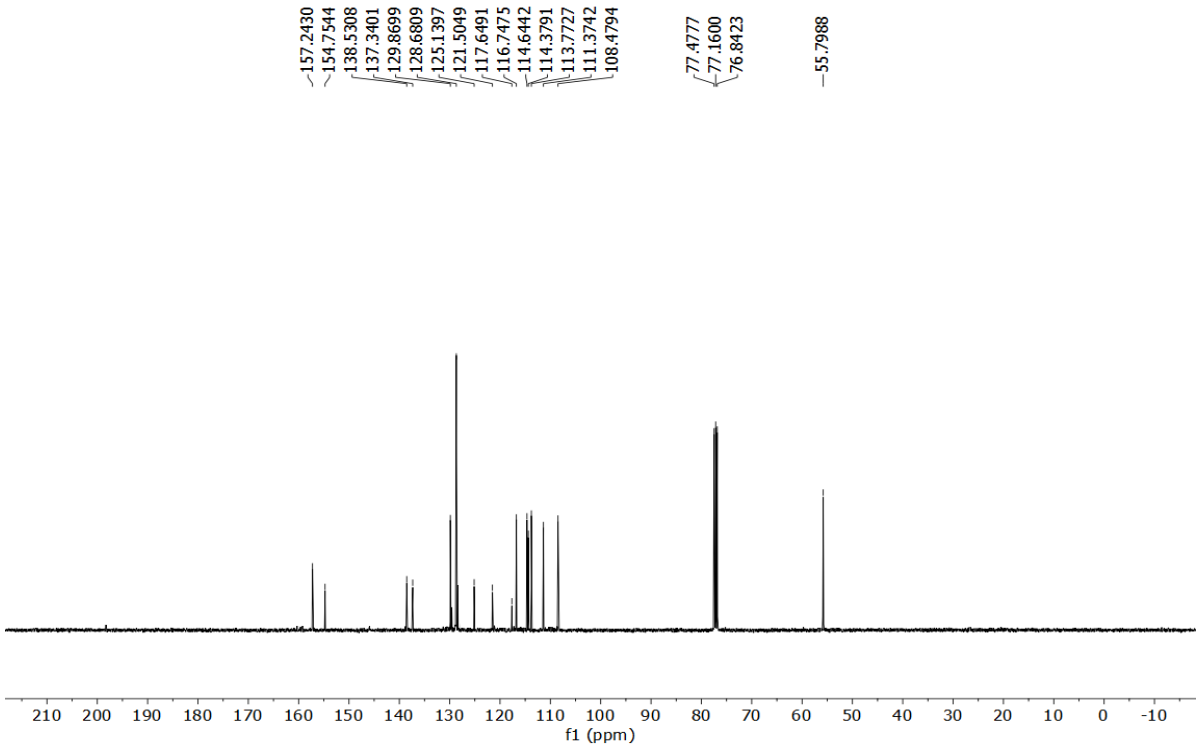

**1-phenyl-9H-pyrido[3,4-b]indole (6a) :**

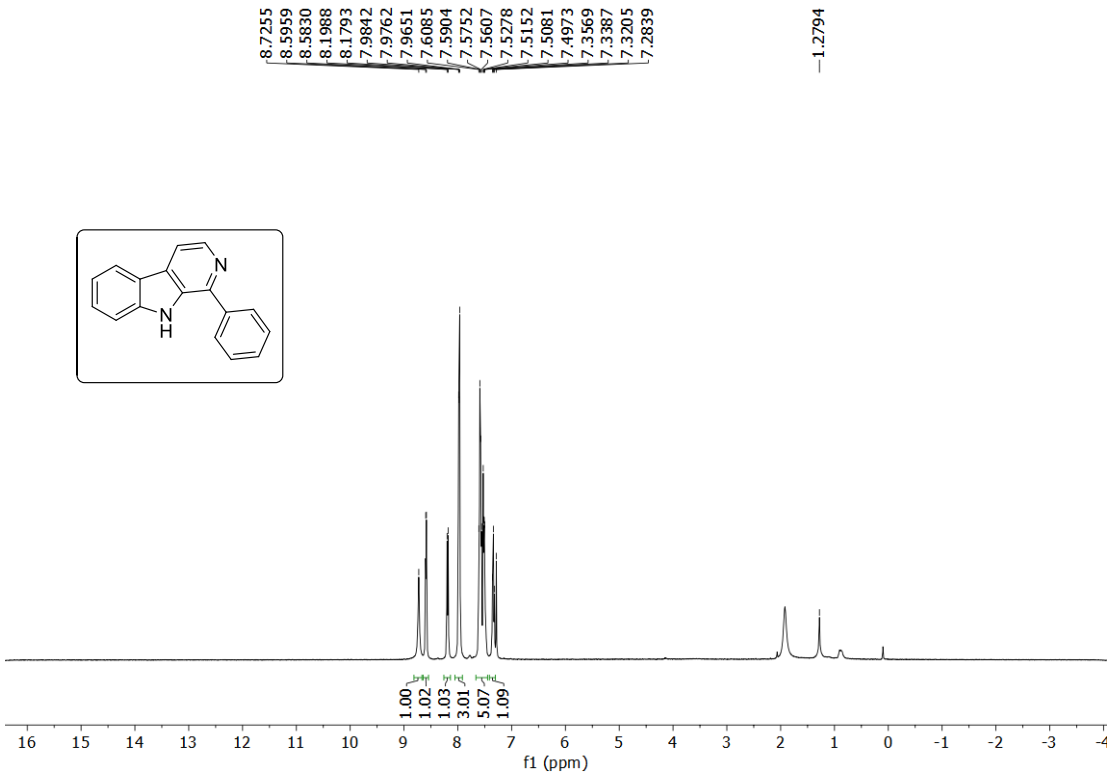


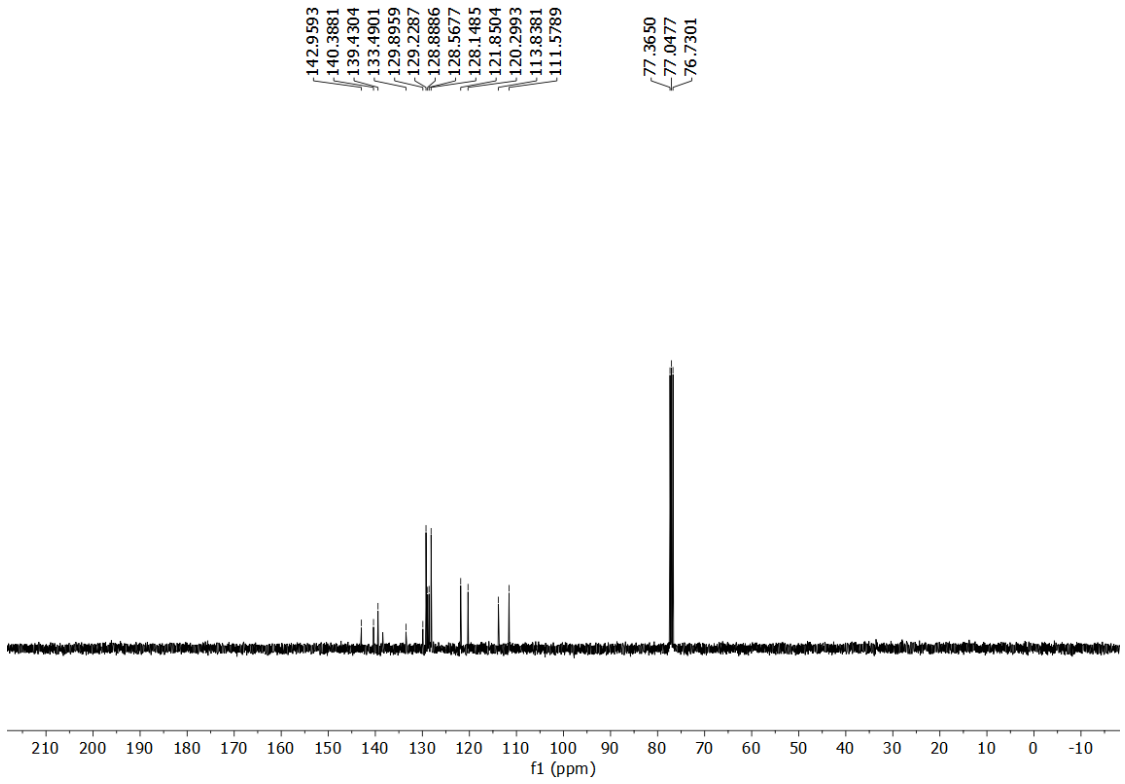

**Phenyl(9H-pyrido[3,4-b]indol-1-yl)methanone (6b) :**

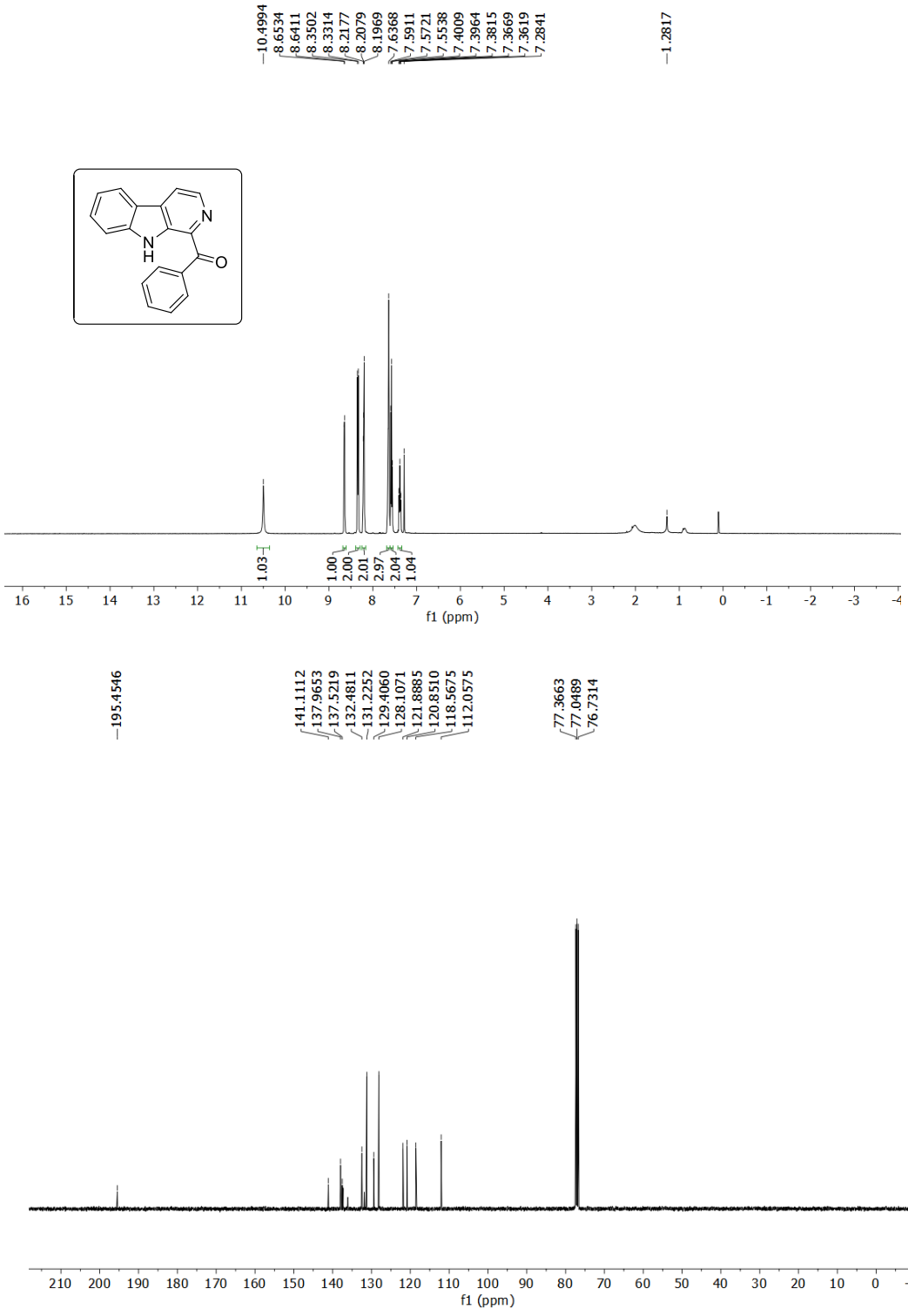

**Methyl 1-phenyl-9H-pyrido[3,4-b]indole-3-carboxylate (6c) :**

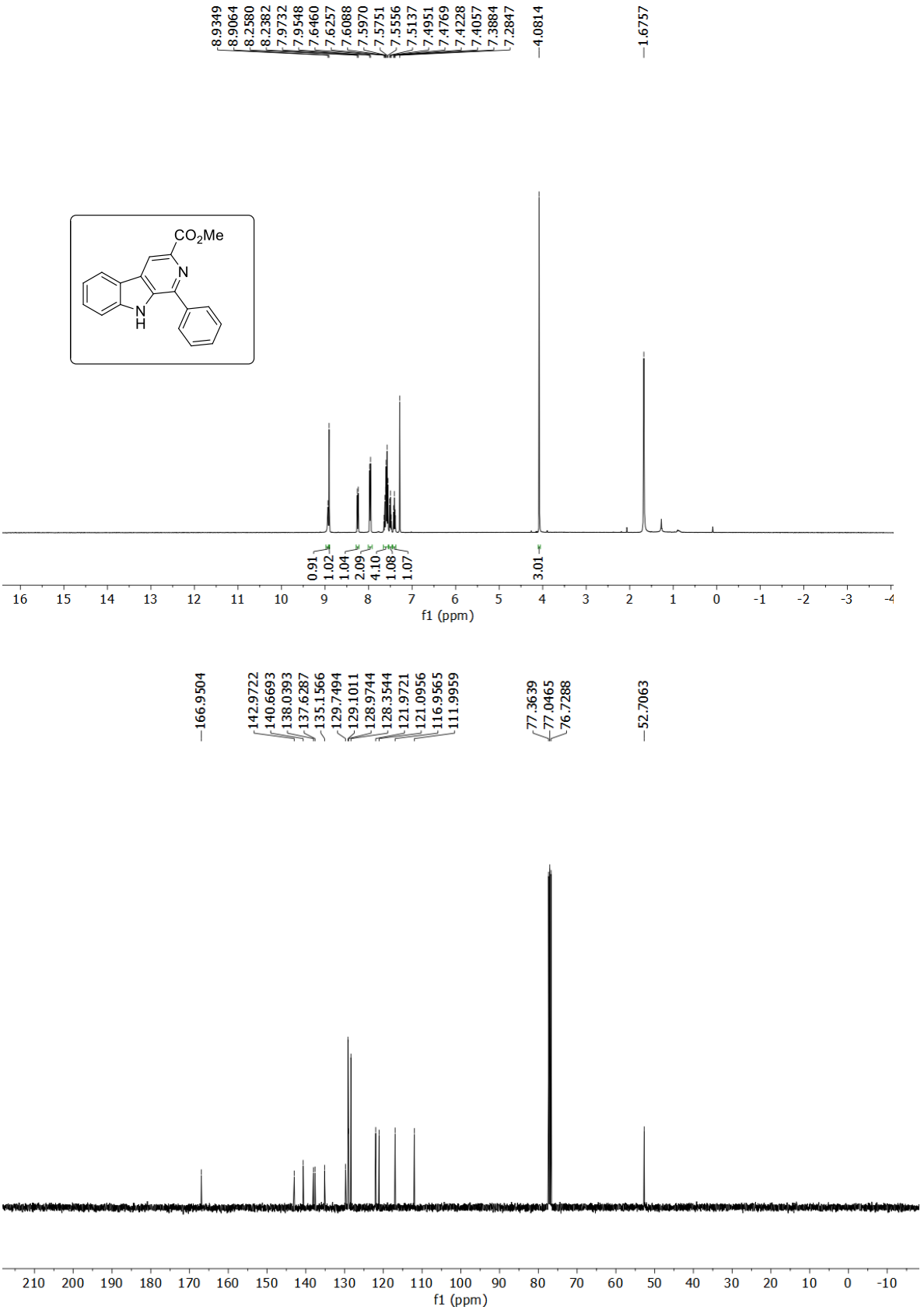

**Ethyl 1-phenyl-9H-pyrido[3,4-b]indole-3-carboxylate (6d) :**